Review article: Fabrication of nanofluidic devices

Chuanhua Duan, Wei Wang, and Quan Xie

View Online   Export Citation   CrossMark

ARTICLES YOU MAY BE INTERESTED IN

CrossMark
click for updates

Review article: Fabrication of nanofluidic devices

Chuanhua Duan,[1,a),b)] Wei Wang,[2,a),b)] and Quan Xie[1]
[1]*Department of Mechanical Engineering, Boston University, 110 Cummington Street, Boston, Massachusetts 02215, USA*
[2]*Institute of Microelectronics, Peking University, National Key Laboratory of Science and Technology on Micro/Nano Fabrication, Beijing 100871, People's Republic of China*

Thanks to its unique features at the nanoscale, nanofluidics, the study and application of fluid flow in nanochannels/nanopores with at least one characteristic size smaller than 100 nm, has enabled the occurrence of many interesting transport phenomena and has shown great potential in both bio- and energy-related fields. The unprecedented growth of this research field is apparently attributed to the rapid development of micro/nanofabrication techniques. In this review, we summarize recent activities and achievements of nanofabrication for nanofluidic devices, especially those reported in the past four years. Three major nanofabrication strategies, including nanolithography, microelectromechanical system based techniques, and methods using various nanomaterials, are introduced with specific fabrication approaches. Other unconventional fabrication attempts which utilize special polymer properties, various microfabrication failure mechanisms, and macro/microscale machining techniques are also presented. Based on these fabrication techniques, an inclusive guideline for materials and processes selection in the preparation of nanofluidic devices is provided. Finally, technical challenges along with possible opportunities in the present nanofabrication for nanofluidic study are discussed. © *2013 American Institute of Physics*. [http://dx.doi.org/10.1063/1.4794973]

I. INTRODUCTION

Nanofluidics is the study and application of fluid flow in channels/pores with at least one characteristic dimension below 100 nm.[1,2] Compared with the well-developed microfluidics, nanofluidics exhibits several unique features, such as ultra-high surface to volume ratio, scales comparable with the range of various surface/interfacial forces, and the size of important biomolecules like DNA or proteins. These unique features give access to many novel transport phenomena that only occur at the nanoscale. For example, the large surface volume ratio results in capillarity-induced negative pressure in water[3,4] and diffusion-limited reaction.[5] The strong electrostatic interaction between charged surface and ions in the nanochannel leads to the formation of overlapped electrical double layers and thereby results in a surface-charge-governed ion transport.[6,7] The proximity of channel feature dimension and size of biomolecules give rise to selective molecule transport and DNA stretching.[8] Inspired by these novel transport phenomena, nanofluidics has already found tremendous applications in many biological fields over the last ten years, including single molecule analysis, biosensing, sample preconcentration/separation, and nanofluidic electronics.[1,9–11] This field is even now expanding to address the critical challenges the macro world is facing. For example, new solutions for energy conversion/storage[12–14] and water purification[15,16] have been proposed based on nanofluidic principles.

It is no doubt that the unprecedented development of nanofluidics is driven by these exciting new transport behaviors and novel applications. However, the most important factor that

---

a)C. Duan and W. Wang contributed equally to this work.
b)Authors to whom correspondence should be addressed. Electronic addresses: duan@bu.edu (Tel.: 617-353-3270) and w.wang@pku.edu.cn (Tel.: 86-10-6276-9183).

promotes the rapid growth of nanofluidics is the fast development of micro/nanofabrication techniques in the same period. In fact, although studies related to nanofluidics have been conducted for centuries in membrane and colloid sciences, the term, nanofluidics, has only been introduced recently with the advances of nanofabrication techniques, which enabled the fabrication of fluidic devices with well-defined nanometer-sized geometries and varied functional materials. These "modern" nanofluidic devices are ideal systems to study and utilize fluidics in a precise manner, which significantly differs from the classic nanofluidic device, i.e., membrane and other mesoporous media, where only statistical results are expected. Present versatile and powerful nanofabrication techniques are able to prepare nanofluidic devices with various dimensions, from 0-D, 1-D to 2-D, categorized based on the number of non-nanoscale dimensions in the key nanostructure component. In the nanofluidic field, 0-D, 1-D, and 2-D nanochannels are generally referred to as nanoporous matrix/nanopores, nanotubes, and nanoslits, respectively. In some cases, short nanotubes with a length less than $10\,\mu m$ are also customarily called nanopores.[17] Nanofluidic devices can also be produced with different channel aspect ratio (AR, the ratio of channel height to width) to meet requirements from diverse applications. 0-D and 1-D nanochannels usually have near-unity AR, while 2-D nanochannels can be either low-AR (planar) or high-AR (vertical) ones. Furthermore, the present nanofabrication techniques have showed a powerful capability of handling a variety of functional materials, from traditional inorganics, such as silicon, glass, and quartz, to organic polymers, like polydimethylsiloxane (PDMS), polymethylmethacrylate (PMMA), etc., which meets the rapid development of nanofluidics studies and applications.

Despite similar definitions in terms of dimension and aspect ratio, fabrication of nanofluidic devices is significantly different from that of regular nanostructures[18,19] as it requires one to form sealed nanoscale hollow channels without collapsing and/or connect these key nanometer-sized components to a supportive fluidic network, usually constructed by microchannels, for sample operations and system integration. Over the last several years, several excellent reviews were dedicated to the fabrication of nanofluidic devices.[9–11,20–23] As many new fabrication approaches have been developed recently and nanofluidic devices have found a wide range of novel applications as mentioned above, an updated review with more comprehensive coverage of nanochannel/nanopore fabrication approaches is highly desired to the nanofluidics community.

In this review, we plan to achieve such a goal by investigating recent activities and achievements of nanofabrication for nanofluidic study, especially those reported in the past four years. It is certainly impossible to include all related publications in this review, and we apologize in advance to any whose efforts may have been left out. In addition, we will also provide an inclusive guideline for materials and processes selection for the fabrication of nanofluidic. This review is summarized and organized as follows. In Sec. II D, three major nanofabrication strategies, including nanolithography, microelectromechanical system (MEMS) technique based nanofabrication, and methods using various nanomaterials, are introduced with specific fabrication approaches. Section V presents several other unconventional attempts to fabricate nanofluidic devices. Afterwards, guidelines for materials and processes selection in nanofluidic device preparation are summarized in Sec. VI. Finally, technical challenges along with possible opportunities in the present nanofabrication for nanofluidic study are discussed in Sec. VII.

II. NANOLITHOGRAPHY APPROACHES

It is well known that the resolution of conventional photolithography is limited by the wavelength of the incident light. Although state-of-the-art photolithography tools in semiconductor industry allow minimum feature sizes down to 22 nm, considering the huge initial investment and expensive running cost, current research facility can only provide patterns with characteristic size around or above $1\,\mu m$ using photolithography, which is much larger than the critical dimension required by nanofluidic studies. It is, therefore, straightforward to employ other available lithography techniques with nanometer resolutions to fabricate nanofluidic devices. To date, several nanolithography techniques including electron beam lithography (often abbreviated as electron beam lithography or EBL), focused ion beam (FIB), nanoimprint

lithography (NIL), interferometric lithography (IL), and sphere lithography (SL) have been developed to beat the diffraction limit of light in standard photolithography. In this section, different nanofabrication methods using these nanolithography techniques are introduced. The first two, EBL and FIB technique are good methods to create single or small scale nanochannels in a direct writing manner. While, the other three, NIL, IL and SL, are usually employed to create large-scale nanopore/nanochannel arrays.

A. Electron beam lithography (EBL)

EBL is a fabrication process of emitting a beam of electrons along a pre-defined path on a surface covered with a thin film of electron sensitive resist and of selectively removing either exposed or unexposed resist thereafter. The purpose, similar to photolithography, is to create small structures in the resist, which can be further transferred to the substrate by reactive ion etching (RIE) or other etching/deposition processes. However, unlike conventional lithography, EBL patterns the resist without masks but in a direct writing mode.[24]

Two major approaches have been developed to fabricate nanofluidic channels using EBL (Figure 1). In the first one, EBL-patterned nanostructures, including patterned resist (usually negative resist such as SU-8[25]) (step a2) and patterned substrate (step a3) such as silicon and silicon dioxide,[26,27] serve as molds for casting PDMS nanofluidic channels (step a4). The resulting open PDMS nanochannels are then bonded to a substrate with the aid of an oxygen plasma treatment (step a5). As PDMS is a hydrophobic material, reagents such as DK Q8-8011 were added to the prepolymer of PDMS to make nanochannel less hydrophobic.[27] Besides, Norland Optical Adhesive (NOA 63), a UV-curable polymer was utilized as an alternative choice of PDMS to cast polymer nanochannels.[26] The second approach generates open nanochannels on the substrates directly (step b2).[28–33] The depth of these open nanochannels can be precisely controlled by RIE because of its slow etching rate. After the etching step, the resist is removed (step b3) and the substrate is bonded with another substrate to seal the nanochannels (step b4).[31–34] Access holes are fabricated by sand blasting on either the cover substrate[31,33,34] or the patterned substrate[32] before the sealing process. More details regarding various bonding techniques can be found in Sec. III B in this review. Besides this bonding based sealing, there are
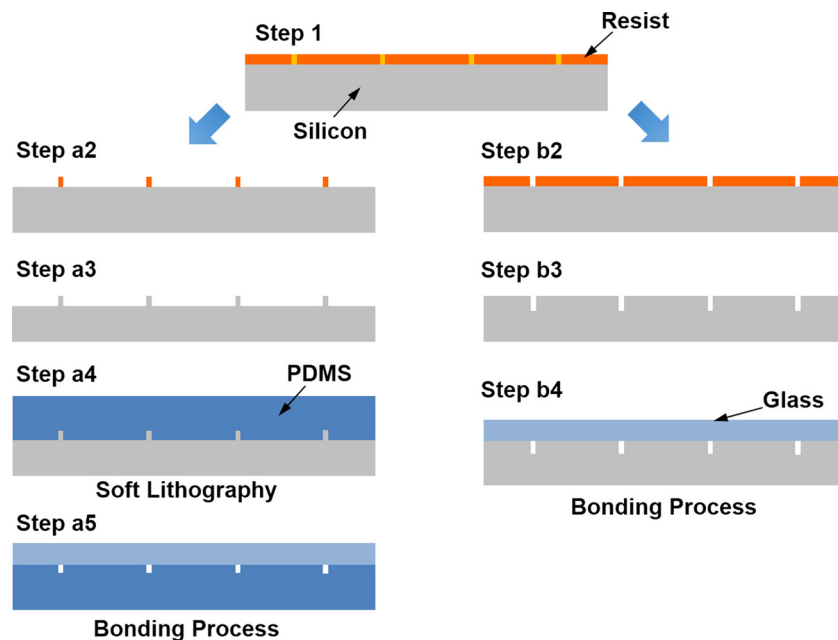

FIG. 1. Schematic of nanochannel fabrication based on electron beam lithography. Step 1: Electron beam exposure. Steps a2-a5: Negative resist patterning, mold etching, soft lithography, and bonding. Steps b2-b4: Positive resist patterning, nanochannel etching and bonding.

several self-sealing methods to form enclosed nanochannels. It has been reported that EBL patterned open nanotrenches can be sealed by atomic layer deposition (ALD) to form sub 10 nm channels.[35] Bilayer e-beam resist, PMMA/PMGI (polydimethyl glutarimide), is also used for self-sealing the channel.[36] After exposed by EBL, the more sensitive PMGI (bottom layer) is fully exposed and developed to form the nanochannel, while the PMMA (top layer) leaves a chain of dot patterns right above the PMGI pattern. Reflowing PMMA produces a polymer nanochannel with channel width defined by EBL.

As electron beam has a much smaller wavelength than UV light in convectional photolithography, features of 10 nm scale or even smaller can be achieved by EBL. Furthermore, EBL is ready for further integration with other traditional microfabrication techniques, such as sacrificial layer releasing (SLR),[37] to prepare complicated micro/nanofluidic devices. However, EBL is not a suitable tool for mass production of nanofluidic devices because of its relatively high cost and low scanning/writing speed.

B. Focused ion beam (FIB) technique

FIB is a technique that utilizes a focused beam of ions to achieve site-specific fabrications, such as swelling, milling, implantation, ion-induced deposition, or etching, with nanometer resolution.[38] It is often known as a powerful defect-repair tool in the semiconductor industry. Recently, FIB, especially FIB milling, attracts great attentions in the nanofabrication because it is capable of generating specific nanoscale patterns directly on hard substrates without requiring masks or photoresists. When FIB is operated with a proper beam size, beam current, and energy (10–100 keV) during a milling process, a cascade of collisions introduced by incoming ions can provide target atoms enough energy to overcome surface binding and escape from the substrate, which thereby leaves nanoscale trench *in situ*.[38,39]

FIB milling is widely used to fabricate nanopores through thin membranes prepared by standard microfabrication.[40–45] Low stress silicon nitride (SiN) prepared by low pressure chemical vapor deposition (LPCVD) is the most used membrane material in this approach (Figure 2).[40–43] Ga+ FIB milling is operated to drill nanoscale ($\sim$10 nm) openings through the SiN membrane (step 2). To prevent surface from charging up due to ion implantation and secondary electrons generation, a metal layer, such as Au and Cr, or conductive polymer is usually coated onto the SiN layer before the drilling process. Electron beam irradiation is an alternative method to compensate surface charging effects. After drilling, ALD is applied to further narrow
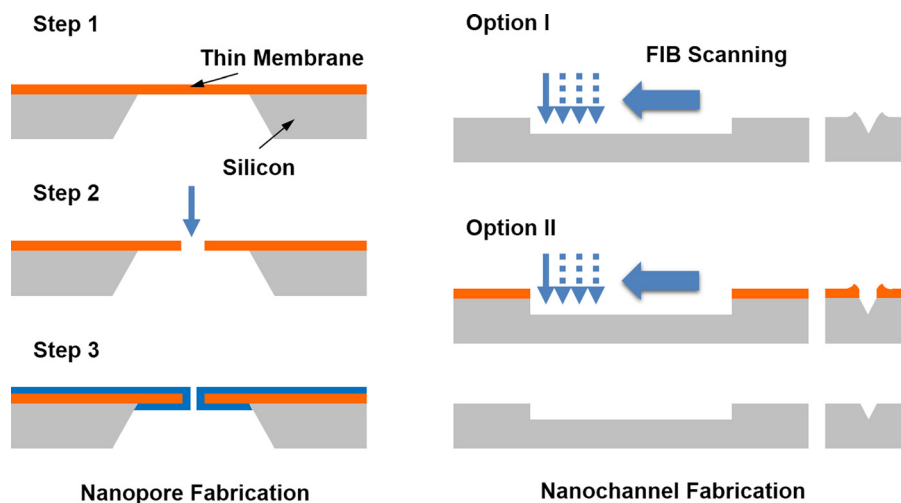
FIG. 2. Schematic of nanopore/nanochannel fabrication based on focused ion beam technology. Nanopore fabrication: Step 1: Thin film deposition and back chamber etching. Step 2: FIB milling. Step 3: Nanopore shrinkage using isotropic deposition. Nanochannel fabrication: Option (I) Direct FIB scanning, Option (II) Introduction of a sacrificial layer, followed by FIB scanning and sacrificial layer etching. The additional sacrificial layer in option II can help remove ridges formed during FIB scanning.

the nanopores (step 3). The additional Al_2O_3 layer can also reduce the electrical noise and thus improve device performance.[40] Similarly, electron-beam-assisted silicon oxide deposition[41] or another ultrathin layer of LPCVD SiN deposition[43] was carried out to reduce the diameter of the nanopore (step 3). Besides SiN, other materials including gold,[46] aluminum,[44] PMMA,[45] and PDMS[47] have been used to form corresponding functional nanopores by FIB milling as well.

Another application of FIB in nanofabrication of nanofluidic devices is to generate nanochannels parallel to the surface using a scanning mode (Figure 2). Nanochannels with feature size of several tens of nanometers have been successfully fabricated by FIB milling on silicon substrate,[48,49] quartz substrates,[50,51] and grown thermal oxide layer[52] (option I). Although etched nanochannels can be sealed by glass wafer through various bonding techniques,[52] the corresponding sealing is not trivial as FIB-milled nanochannels usually have ridges along the channel banks due to swelling and re-deposition during milling[53] (option I). Such ridge structures can be avoided by introducing a sacrificial layer (a relatively thick metal film) onto the target substrate before milling and then selectively removing it afterwards (option II). 1-D open nanochannels with smooth top surfaces and lateral dimensions as small as sub-5 nm were fabricated based on this approach, which were easily sealed with a cover plate.[51]

FIB technique has also been utilized to fabricate multi-functional micro/nanofluidic devices on silicon wafers when it was integrated with traditional micromachining processes. For example, nanofluidic devices with embedded transverse nanoelectrodes were successfully fabricated using combined techniques including photolithography, silicon etching, lift off, FIB Pt deposition, and milling.[52] Another example is milling the substrate with predefined microstructures to prepare hybrid micro/nanoscale molds for soft lithography based micro/nanochannel fabrication, which can lower down the cost for massive production of nanofluidic devices.[54–56]

In short, FIB has shown its promise in the fabrication of nanofluidic devices as it can directly generate nanoscale features on the substrate and is compatible with other fabrication techniques. Unfortunately, this technique still requires costly equipment and the fabrication yield is even lower than EBL because of the direct milling/deposition mode.

C. Nanoimprint lithography (NIL)

In addition to the above two direct writing based techniques, NIL is an important nanolithography method with high-throughput capability. Unlike conventional lithography, NIL replicates nanoscale features by mechanically pressing predefined molds into imprint resist and thus overcomes the diffraction limit.[57] It has been widely used in recent decades to fabricate 1-D and 2-D nanochannels in varied nanofluidic systems.

As shown in Figure 3, in a typical NIL-based nanochannel fabrication process, a thin layer of imprint resist is first spun onto the substrate (step 1). A hard mold with predefined nanoscale patterns is then brought into contact with the substrate and they are pressed together under certain load (step 2). Subsequently, the resist layer is cured and solidified by heat or UV light. The pressure and temperature during this imprinting (pressing and curing) step are carefully controlled to achieve robust mechanical deformation of the imprint resist. After the curing process, the hard mold is removed, leaving the reverse nanostructures on the resist layer (step 3). This patterned resist can directly function as open nanochannel (step 3) or serve as a mask for pattern transfer to fabricate the open nanochannel. In the latter case, the residual resist remaining in the contact area is removed by O_2 plasma etching first (step 4) and then another etching step transfers the nanopattern onto the substrate. Similar to other nanolithography-based nanochannel fabrication approaches, the NIL-based approach also requires a sealing/bonding step to enclose the open nanochannels. Direct thermal bonding with polymers including SU-8[58,59] and PMMA[60] has been utilized as one of the popular sealing/bonding methods. Solvent vapor sealing[61] and melting induced reflowing[62] have also served as promising methods in sealing the NIL prepared nanochannels. In addition, the NIL template itself can be directly used to form enclosed nanochannels between imprint resist and the template if the deformed imprint resist cannot completely fill the trench region on the template.[63] Although this method is a single-step process for nanochannel
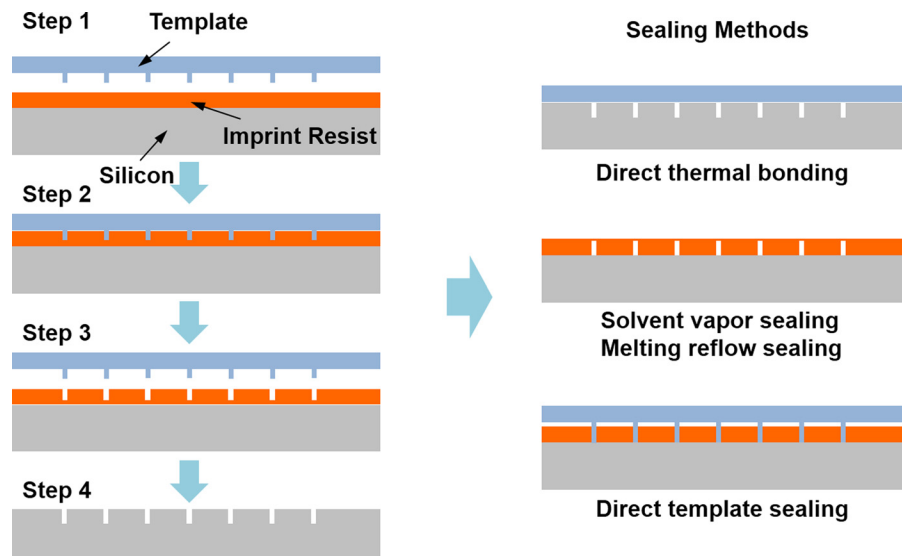
FIG. 3. Schematic of nanochannel fabrication based on nanoimprint lithography. Typically, this method includes two major processes, i.e., nanochannel patterning and nanochannel sealing. The patterning process consists of four steps: Step 1: Imprint resist coating. Step 2: Mold pressing. Step 3: Mold removal. Step 4: Residual resist etching. Available sealing options include direct thermal bonding, solvent vapor sealing, melting reflow sealing, and direct template sealing.

fabrication, the imprinting template cannot be reused thereafter, thus losing the main advantage of NIL in nanofabrication.

A variety of materials, such as SU-8,[58,59] PMMA,[60,64] sol-gel silica,[65] and some UV curable polymers,[66] have been employed as imprinting resist. In contrast to the various choices for resist materials, imprint molds are generally made by silicon or quartz because of their stiffness and process compatibility. Silicon/quartz molds can also avoid thermal expansion mismatch with substrates in the imprinting process as in most cases substrates themselves are silicon. Imprint molds used in NIL are generally formed by another nanolithography process (e.g., deep UV lithography, EBL, or interferometric lithography) followed by a corresponding reactive ion etching.

NIL can generate nanoscale features ($\sim$10 nm) over a large area with relatively low cost compared with the aforementioned EBL and FIB as its molds can be reused, which makes this technique promising in high-throughput nanofluidic device fabrication. Another advantage of the NIL-based nanochannel fabrication is its compatibility with other microfabrication approaches in terms of forming complicated micro/nanofluidic devices. For example, mixed-scale structures were prepared by employing NIL on a pre-processed substrate with microstructures on top.[64] Reano and Pang have developed sequentially stacked thermal nanoimprint lithography on planarized layers to achieve multi-level (3D) nanochannel network on a silicon wafer.[67] Two sequential NIL (Dual-NIL) processes have recently been advanced to fabricate electrodes over nanofluidic channel for *in situ* DNA transportation detection.[68] Hierarchical silica nanochannels have also been fabricated by introducing block copolymer thin film template.[66] In spite of these advantages listed above, NIL may not be a cost-effective nanolithography technique when imprints molds are not available or only used for limited times as the fabrication of the imprints modes requires other expensive nanolithography techniques.

D. Interferometric lithography (IL)

Similar to NIL, IL is a technique capable of fabricating large-area, nanometer-sized, periodically patterned structures.[69] In the literature, this technique has been variously referred to as holographic lithography, or interference lithography. In this technique, a coherent laser source is split into two different beams and then projected onto the photoresist. Typical sinusoidal interference pattern with certain pitch is formed on the photoresist based on interferometric

exposure of these two coherent beams. The resulting patterning line width is determined by the incident light wavelength, angle, and developing time. This process is maskless and only relies on light and material properties. Nanoscale pattern of the photoresist can be transferred to the substrate via etching process. Up to now, the width of nanochannel immediately after etching can reach 200 nm and further thermal oxidation may narrow the width down to 100 nm or smaller.

Researchers have employed this method to fabricate large scale nanochannel array on silicon substrate.[70–76] IL can also be used to fabricate nanoscale molds, which can serve as masters for PDMS molding to fabricate PDMS nanochannels.[77] In addition, combining with traditional MEMS techniques, IL has been used to pattern high-density nanopore array with porosity of approximately 20%.[78] Multilayer fluidic platform was achieved by sandwiching this nanopore membrane with other PDMS microfluidic networks.[79] However, IL can only generate nanochannel/nanopore array based on its working principle. The inability to fabricate single nanochannel/nanopore limits its applications in nanofluidics.

E. Sphere lithography (SL)

SL, also named as colloidal lithography, is another low-cost technique to pattern large-scale two dimensional ordered nanostructure arrays,[80–82] especially nanopore arrays. As shown in Figure. 4, to fabricate a nanopore array based on SL, a close-packed nanoparticle monolayer is first prepared on a plane substrate (step 1). These close-packed nanoparticles are used as an etching mask to transfer triangular interstice patterns into the substrate by a subsequent anisotropic etching (step I2).[83] Or, they are separated by a controlled reactive ion etching (step II2) and then covered with metal or other thin film materials (step II3). After releasing the residual nanoparticles, hole-shaped nanopatterns are left on the substrate, as indicated in step II4. The nanohole patterns in the deposited film can be directly used as a nanoporous membrane after an
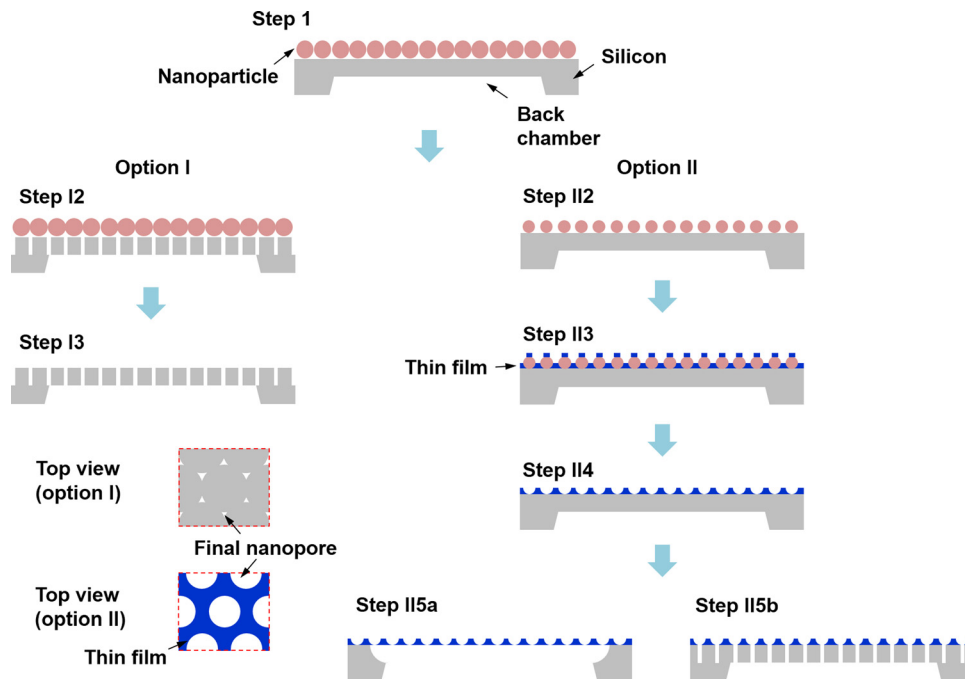
FIG. 4. Basic fabrication process of nanopore array by sphere lithography. After the preparation of a close-packed nanoparticle monolayer (step 1), two fabrication approaches are available and lead to different final structures. Option I: Step I2: Dry etching the substrate. Step I3: Releasing nanoparticles. Option II: Step II2: Dry etching the nanoparticles. Step II3: Depositing thin film. Step II4: Releasing nanoparticles. Step II5a: Isotropically etching the substrate. Step II5b: anisotropically etching the substrate. Substrate with a pre-etched back chamber was used here. The back chamber can also be created after step I3 or step II5 to form the final structure.

isotropic etching of the substrate (step II5a), or can be further transferred into the substrate with an anisotropic etching (step II5b). The latter step can be used to form a suspended membrane with a through-nanopore array, once a back chamber is prepared by the traditional microfabrication technique either before the sphere lithography or after.

The key step in the SL based nanofabrication approach is the preparation of a high quality monolayer of nanoparticles. Most monolayers are formed by classic assembly-based methods, including evaporation induced self-assembly,[84] Langmuir-Blodgett deposition[85,86] or roll-to-roll process.[87] Even some of the above methods[86,87] have demonstrated their ability in wafer-scale fabrication, the process compatibility of the assembly-based nanoparticle monolayer preparation with traditional microfabrication still remains a challenge due to requirements of special instruments and tricky manual operations, which limit the applications of sphere lithography in nanofluidics. Recently, monolayer of nanoparticles has been achieved by spin-coating a photoresist or hybrid sol[88] with particles doped. These new methods, in principle, are compatible with traditional microfabrication processes and thereby hold great potential in developing another useful tool for the fabrication of micro/nanofluidic devices.

III. MEMS BASED NANOFABRICATION APPROACHES

Although nanolithography based approaches can fabricate various nanostructures, the most popular nanofabrication approaches still rely on standard MEMS techniques due to their high throughput and low cost, benefiting from the wafer-scale processing ability. These MEMS based fabrication approaches usually involve structure definition using standard photolithography and structure formation via a series of additive (deposition)/subtractive (etching) processes. Although conventional photolithography tools in a research facility cannot directly define nanoscale features, precise controls in the well-defined deposition/etching processes can create structures with depth and/or width in the nanoscale. In the following section, we will introduce five different MEMS based fabrication approaches. The first two, sacrificial layer releasing and etching and bonding are usually used to fabricate 2-D planar nanochannels with a low AR. The other three, including etching and deposition, edge lithography, and spacer technique, are more suitable for fabricating 2-D vertical nanochannels with a high AR.

A. Sacrificial layer releasing (SLR)

SLR is one of the most popular top-down approaches to fabricate 1-D or 2-D nanochannel devices. In this process, nanochannels are formed with a nanometer-thick sacrificial layer that is first used to define the male form of the nanochannel and is then removed in order to open the aperture[21] (Figure 5). Generally, a bottom layer is deposited on the substrate (step 1),
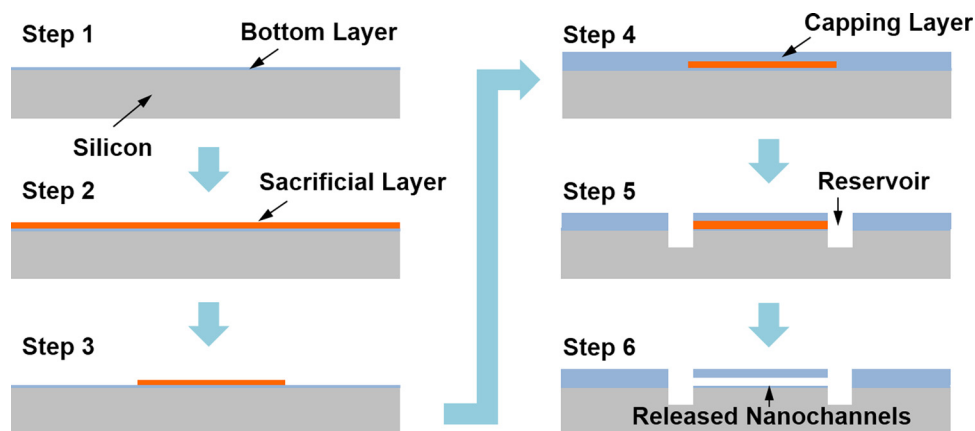

FIG. 5. Schematic of nanochannel fabrication based on sacrificial layer releasing method. Step 1: Deposition of the bottom layer. Step 2: Deposition of the sacrificial layer. Step 3: Pattern sacrificial layer to create the male form of the nanochannel. Step 4: Deposition of the capping layer. Step 5: Formation of access reservoirs. Step 6: Nanochannel releasing.

followed by the deposition of a thin sacrificial layer (step 2). After patterning this sacrificial layer (step 3), a capping layer is deposited to enclose the patterned structures (step 4). The capping layer is then patterned to make holes for etchant later to access the sacrificial layer (step 5). Finally, the sacrificial layer is removed using a selective etching process to form the nanochannels (step 6). It is the thickness of this sacrificial layer that determines the height of the nanochannel. The bottom layer (step 1) is not always required, but is usually introduced to make the channel of the same material.

The commonly used sacrificial materials are amorphous/polysilicon,[3,6,89–95] silicon dioxide,[96,97] metals,[98–105] and polymers.[106–114] Among them, amorphous/polysilicon[3,5,89–95] and silicon dioxide,[96,97] were chosen first due to their temperature stability, mechanical rigidity, and process compatibility with the subsequent deposition processes. The corresponding etchants are xenon difluoride (XeF_2, dry etching of silicon)/tetramethylammonium hydroxide (TMAH, anisotropic wet etching of silicon), and hydrofluoric acid (HF, wet etching of silicon dioxide), respectively. Metals are also a class of popular sacrificial materials. The high selectivity of the metal etchant (up to 10^6:1) between metal and substrate ensures excellent height uniformity throughout the whole channel. So far, Al,[98,99,103] Cr,[100–102,105] Ge,[94,104] Ti/W,[100] Pt,[100] Cu,[100,105] and Ta[100] have been tested to produce nanofluidic channels. In addition to these inorganic materials, several organic polymers, including SU-8,[99] Shipley S1805 photoresist,[106] polyvinyl alcohol (PVA),[107] polyethylene oxide,[108,109] polynorbornene,[112,113] polycarbonate (PC),[114] and even DNA[110,111] have also been used as sacrificial materials. However, compared with inorganic materials, there are limited choices of capping materials for these polymers.

Although lots of materials can serve as the sacrificial material, the traditional SLR approach suffers from slow, diffusion-limited etching, making it difficult to produce long nanochannels. It has been reported that releasing a 0.66-mm long nanochannel would require 15 h of etching.[3] One way to reduce the etching time is to release the sacrificial layer from its side instead of from two ends. A subsequent non-conformal deposition, e.g., plasma-enhanced chemical vapor deposition (PECVD), can reseal the channel from the side to prevent leakage. Because etching from the side is along the channel width direction instead of the channel length one, this alternative approach could significantly save the etching time. Huang *et al*. have used this method to prepare centimeter-long nanochannels within 90 s.[115] One drawback regarding this method is the edge deformation of the capping layer due to stress release during etching.[115] Consequently, the cross-section of the final released nanochannel deviates from the originally designed rectangular shape. This issue becomes less serious when thick capping layer is deposited and/or the etching period is well controlled to have a very short releasing path.[104] The latter case has actually been developed as a new method to fabricate 1-D nanochannels. Hoang *et al*. used this method to produce 10 mm-long 1-D nanochannels with a cross-section of 20 nm × 40 nm.[116] By carefully controlling the side etching time, Sordan *et al*. have also created nanochannels with a cross-section of 10 nm × 10 nm.[104] Another alternative approach to shorten the releasing time is to use new sacrificial materials that are easy to remove. Thermal decomposable polymers[112–114] were introduced as a new class of sacrificial material for this purpose. These polycarbonate-based polymers vaporize when they are heated up to certain temperatures (300–400 °C), yielding short releasing time due to fast gas diffusion. These polymers are also sensitive to E-beam irradiation and thus could be used as resist for nanoscale patterning and fabrication of 1-D nanochannels. Despite these advantages, it is worth noting again that there are limited choices of the capping layers since most deposition of the capping layer has a process temperature higher than the glass temperatures of these polymeric sacrificial materials. In addition to these two approaches above, new etching methods can be applied to speed up the releasing process. For example, external electric potential has been applied to accelerate galvanic corrosion during the releasing Cu/Cr sacrificial layers.[100,105]

While SLR is mostly used to fabricate single or a small group of horizontally aligned 1-D/2-D nanochannels, it also has the potential to form large scale nanofluidic structures. Grattoni *et al*. have used sacrificial layer etching to prepare densely packed nanoslits (nanofluidic membranes) with 5.7 nm and 13 nm in height.[117] James Lee's group has combined this technique with imprinting to form laterally ordered nanochannels arrays using DNA wires as the

sacrificial structures.[110,111] They also used a similar approach to prepare conical shaped nano-pore array with PVA as the sacrificial material.[107] Besides horizontal nanochannel array, sacrificial layer releasing has also been employed to generate vertically aligned nanochannel arrays by multi-step deposition of sacrificial and capping layers. Shen *et al.* alternatively deposited multilayers of silicon nitride (capping layer) and silicon oxide (sacrificial layer) to achieve nanofiltration structures with minimum channel height of 100 nm.[97] Sordan *et al.* fabricated vertical nanochannel array by selective side etching of a SiGe heterostructure comprised of layers of alternative Ge fraction.[104]

In short, compared with other nanochannel fabrication approaches, SLR is relatively simple and inexpensive, amenable to integration with other microstructures to form integrated micro/nanofluidic devices and capable of fabricating complicated 3-D nanofluidic structures. The formed nanochannels are only several microns (or even less) from the device surface, allowing accurate observation and interpretation of the experiments. However, this surface micromachining approach has two inherent limitations. First of all, it is difficult to use this approach to fabricate ultrathin nanochannels. Current minimum channel size using this approach is around 10 nm, below which it is difficult to control the thickness of the sacrificial layer and channel tends to collapse due to capillary force during etchant extraction or liquid introduction. Such collapsing during releasing can be intentionally introduced to form 1-D nanochannels.[94,118] Secondly, etchants and reactants may remain inside the (long) channels after releasing, resulting in undesirable influence on the subsequent nanofluidics experiments.[116]

B. Etching and bonding

Another commonly used MEMS fabrication approach for nanofluidic devices is etching and bonding. In this approach, 2-D planar nanochannels are formed by etching nanometer-deep trenches in a substrate, followed by bonding it to another plane substrate (Figure 6). Normally, this fabrication scheme starts with a standard photolithography step on a double-side polished silicon or glass (quartz) substrate. This photolithography is used to define the width and length of the nanochannel. Using the patterned photoresist as a mask, an etching step is then performed to form a shallow trench on the substrate (step 1). It is this etching step that determines the final height of the nanochannel. After this step, similar photolithography and etching are applied again to create microchannels that are used to introduce liquid and connect other fluidic components (step 2). The top surface is then deposited with a thick oxide layer using PECVD (step 3). This layer serves as a protection layer for both microchannels and nanochannels during the subsequent
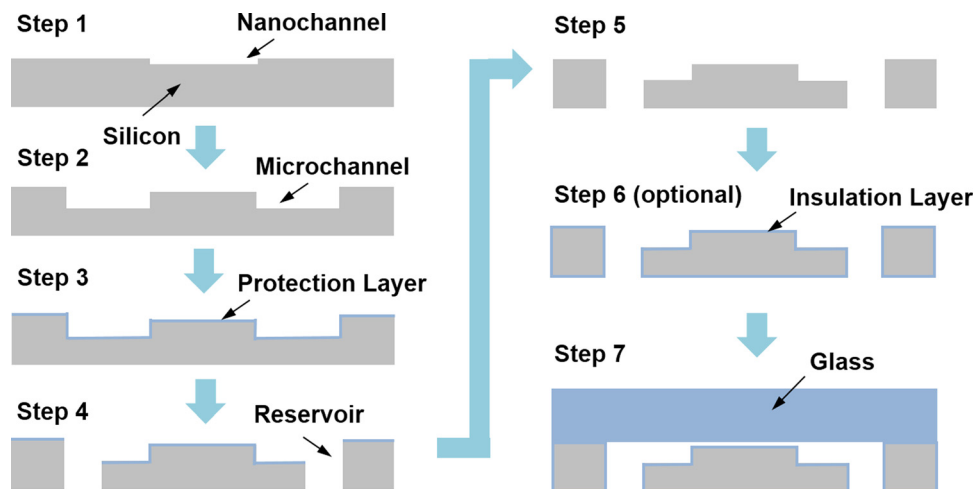
FIG. 6. Schematic of nanochannel fabrication based on etching and bonding method. Step 1: Nanochannel patterning and etching. Step 2: Microchannel patterning and etching. Step 3: Deposition of the protection layer. Step 4: Backside reservoir patterning and etching. Step 5: Removal of the protection layer. Step 6: Uniform growth/deposition of an insulation layer, e.g., a thermal oxide layer (optional). Step 7: Anodic bonding with a glass substrate.

reservoir formation step (step 4). Reservoirs are patterned from the back side of the wafer and a deep reactive ion etching (DRIE) or drilling process is employed to create through-substrate holes. The top oxide layer is removed by HF solution after this step (step 5). The wafer is then sent into a furnace to uniformly grow thermal oxide on all exposed surfaces (step 6). This re-oxidation step is not required, but is usually introduced to add an insulation layer on silicon substrate. Finally, this substrate is bonded with another substrate (step 7) after a careful cleaning process (usually including hot piranha treatment, di-ionized water rinse, and nitrogen blow dry).

As self-explained by its name, there are two major challenges regarding this MEMS-based nanofabrication approach. The first one is the nanochannel etching. Etching techniques with robust and high precision control are desired to achieve nanometer-sized depth. The corresponding etching methods include bulk etching and thin film etching. In bulk etching, the thickness of the trench is determined by the etching rate along with the etching time. Currently, there are two bulk etching techniques, dry etching (usually RIE) and wet (chemical) etching. RIE is mainly used for silicon substrate.[13,119–126] The corresponding etching rate can be adjusted by several parameters in this technique, including gas composition, pressure, power, substrate to electrode distance, and substrate temperature. Although it was initially believed this technique did not have precise controllability and often resulted in a rough etched morphology, advanced RIE technique has showed the ability of etching 2-nm deep trench in silicon with a surface roughness around 0.2 nm.[125] Compared with RIE, wet etching does not have any other tuning parameters for the etching rate except chemical concentration and bath temperature. However, it is much easier to prepare and does not require any special instruments. Wet etching has been used for both silicon and glass substrates. In particular, diluted HF and buffered HF (BHF) have been used to etch glass substrate,[127–135] while NaOH/KOH, TMAH, and Olin OPD 4262 (a positive resist developer) have been used to etch silicon substrate[119,136–138] to form desired nanochannels. In contrast with bulk etching, the depth of the trench in thin film etching is normally predefined by the thickness of the deposited film (spacer layer) once a highly selective etching method is chosen. Various materials, including amorphous silicon,[139–141] poly-silicon,[142] silicon carbide,[143] and silicon dioxide,[118,144–146] have been used as the spacer layer. A special technique under the category of thin film etching is the double thermal oxide technique. In this technique, a thick layer of thermal oxide layer is first grown on silicon substrate. The following selective etching defines the nanochannel horizontal geometry (width and length) and opens a window to expose the underneath silicon substrate. A second thermal oxidization step is then performed to grow a thinner thermal oxide on the exposed regime. The final height of the nanochannel can be determined either by the difference between two oxide layers directly[147] or the consumptions of silicon during the second oxidation on the exposed and unexposed regimes.[148–152] This technique benefits from the precision control of thermal oxide growth and can potentially produce nanochannels with any specified height. Another special technique of thin film etching is to use native oxide (~1 nm) as the spacer layer.[153] Because native oxide can re-grow in ambient atmosphere, the selective etching and re-growing can happen several times to get channels with different heights. 6-nm-deep nanochannels have been created by this method.[153]

Overall, it is no exaggeration to say that current etching techniques are capable of providing precision down to 1 nm. The real limiting step for the etching and bonding approach is, thus, the bonding step. Current available bonding methods include anodic bonding, thermal fusion bonding, as well as adhesion bonding. Anodic bonding is a unique bonding technique that can generate a permanent chemical bond between silicon and glass substrates. This technique requires a high DC voltage (~1000 V) to drive O^{2-} ions moving from glass substrate to silicon substrate to form Si-O bonds at a temperature (~ 400 °C). As a result, nanochannels made by this technique are subject to collapsing due to the strong electrostatic force during bonding. Typically, for a give channel width w, the minimum channel height (h_{min}) that is allowed to avoid collapse follows an expression below:

$$h_{min} = \left(\frac{w \varepsilon_0 V^2}{E_{eff}} \right)^{\frac{1}{3}},$$

where ε_0 is the dielectric constant, E_{eff} is the effective Young's modulus, and V is the applied voltage.[154] One way to overcome this limit is to apply anodic bonding with lower temperature and lower voltage. Song and Wang have used anodic bonding under a condition of 225 °C and 400 V to create nanochannels that were 6-nm-deep and 3-μm-wide.[153] Another alternative method is to intentionally grow a thick insulation layer on the silicon substrate. This insulation layer does not only prevent electrical leakage from channel wall but also serves as a big capacitor and thus reduces electrostatic force during bonding.[125,136] Mao and Han made channels that were 25 nm deep and 4 μm wide using this modified anodic bonding method.[136] Recently, Duan and Majumdar further pushed the limit down to 2 nm deep with the introduction of a 500 nm thermal oxide.[125] Thermal fusion bonding is another important bonding method in MEMS. In this method, two stacked substrates are heated to a high temperature close to their glass transition point. The strong diffusion and local plastic deformation at the interface result in a strong physical bonding. Thermal fusion bonding normally takes longer time than anodic bonding and it only works for substrates with similar thermal expansion coefficients. Otherwise thermal mismatch issue would arise and lead to cracks or even bonding failure. Collapsing is still an issue for fusion bonding, although not as critical as for anodic bonding. 20-nm-deep nanochannels have been achieved using regular glass-glass fusion bonding.[136] This technique can be further improved by using water or manually pressing to pre-bond two substrates together. Haneveld *et al.* used such a modified fusion bonding technique and pushed the channel depth limit of fusion bonding down to 5 nm.[155] In addition to these two bonding methods above, adhesion bonding can also be applied as long as the thickness of the adhesion layer is smaller than the height of the nanochannel. Sodium silicate has been used as such an adhesion agent.[7,135,156] For example, nanochannels down to 50 nm have been formed using uniformly spin-coated, 20-nm thick sodium silicate as the adhesion layer.[135]

In brief, etching and bonding approach is probably the best MEMS based fabrication approach for 2-D planar nanochannels with small AR. This approach is relatively simple and cost-effective; flexible for integration with other fluidic/electrical components; capable of fabricating ultra-long, ultra-thin, and ultra-low AR individual 2-D nanochannels as well as complicated micro/nanofluidic networks.[150,151,157,158] However, there are two minor disadvantages that prevent it from being an ideal nanochannel fabrication approach. One is that all current bonding techniques require extremely clean and defect free surfaces, which adds facility requirements and results in low bonding yield, especially for the fabrication of ultra-thin nanochannels with ultra-low AR. Another concern is that the materials used in this fabrication approach may bring certain application limits: Silicon is not a transparent material and thus may cause background issue for optical observation; glass can gradually dissolve in aqueous solutions and therefore channels may not be reliable for long-term operation.[10,159]

C. Etching and deposition

The nanochannels fabricated by SLR or etching and bonding approaches are mostly 2-D planar channels with nanometer scale height. There are also MEMS based approaches to fabricate 2-D vertical nanochannels with a nanometer-sized width.

One of the approaches is called etching and deposition. This approach is similar to the etching and bonding approach in which open trenches are first formed on the substrate using photolithography and etching. However, instead of forming shallow trenches with nanometer scale height, relatively deep and straight trenches (~at least several microns in depth) are created in this approach using anisotropic etching. A non-conformal deposition step is then exploited to create self-sealing nanochannels, as shown in Figure 7. Clearly, this non-conformal deposition is the key step for this fabrication approach and it has two important functions, i.e., shrinking the trench width to the nanometer scale and sealing the open trenches. It has been reported that both chemical vapor deposition (CVD) and physical vapor deposition (PVD) processes, depending on the operating conditions, can form such non-conformal deposition.[160–163] Specifically, Ilic *et al.* exploited this etching and deposition approach to produce Parylene C nanochannels down to 100 nm regime based on a Parylene C CVD process.[160] Wong *et al.*
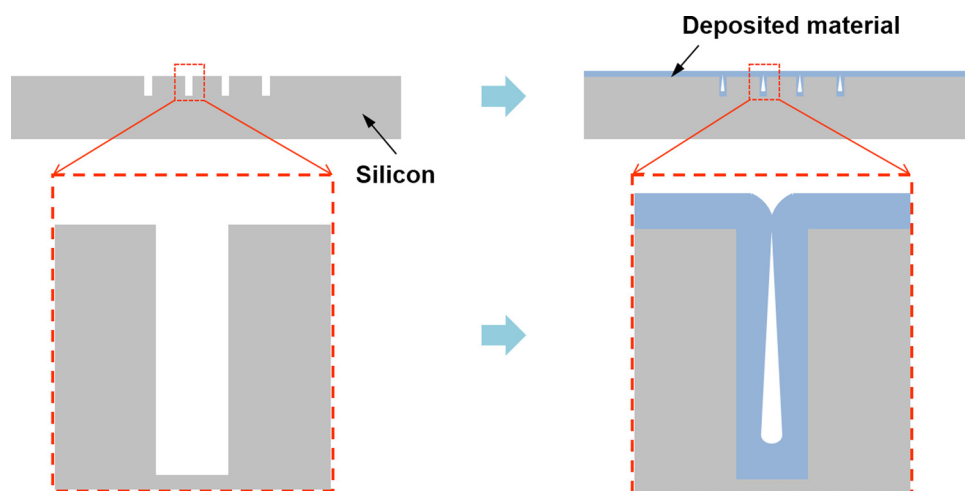
FIG. 7. Schematic of nanochannel fabrication based on etching and deposition method. Non-conformal deposition results in self-sealing nanochannels.

used non-conformal PECVD to seal silicon oxide trenches on silicon wafers with phosphor silicate glass (PSG).[161] They then further modified these nanochannels into circular profiled-nanochannels with diameter ranging from 30 to 2000 nm by reflowing the deposited PSG during a high-temperature annealing process.[161] Mao and Han also used non-conformal PECVD to seal vertical silica nanochannels with channel width down to 50 nm, which was shrunk by a conformal thermal oxidization from an initial width of 500 nm.[163]

Important features of this approach include relatively low fabrication cost and channel self-sealing. Moreover, as 2-D vertical nanochannels are formed below the surface of the substrate, in principle, the top surface is available for further integration of other fluidic components or electronic circuits. This leads to more efficient use of the substrate and improved miniaturization of the overall device.[20] However, despite of the above advantages, this approach lacks precise control on the final channel width due to the complicated non-conformal deposition inside the trench.

D. Edge lithography and spacer technique

Instead of using controlled deposition techniques to shrink the channel width to the nanoscale, 2-D vertical nanochannels can also be formed using controlled etching. Edge lithography technique, where nanoscale features are created by well-controlled undercuts, is one of the representatives[164–166] (Figure 8). To prepare 2-D vertical nanochannels, a thin metal layer (10–100 nm) is first deposited on the substrate and patterned by standard lithography (step 1). Masked by the photoresist, the metal layer is then isotropically etched by a selective metal etchant, resulting in nanometer scale undercuts (step 2). Afterwards, a second metal layer with similar thickness is deposited on the substrate (step 3). A following lift-off process then removes the photoresist along with the metal layer above (step 4). As a result of this step, a metal mask with patterned nanogaps is formed on the substrate. This mask is used in the next DRIE step (step 5) to create deep trench with nanoscale width. Finally, the metal mask is removed (step 6) and nanochannels can be formed by bonding or deposition methods (step 7), similar to what have been introduced in Sec. III B and III C. This technique can also be modified to prepare nanometer-sized molds to make vertical PDMS nanochannels.[165]

Currently, two types of metals, chromium and aluminum, have been used to form the mask with nanogaps for the following DRIE. Other metals and materials can replace these two metals as long as there are corresponding selective and controllable etchants. The typical width of the nanogaps and the resulting nanochannels is around 50–200 nm, which is limited by the undercutting controllability. However, this width can be further reduced by uniformly
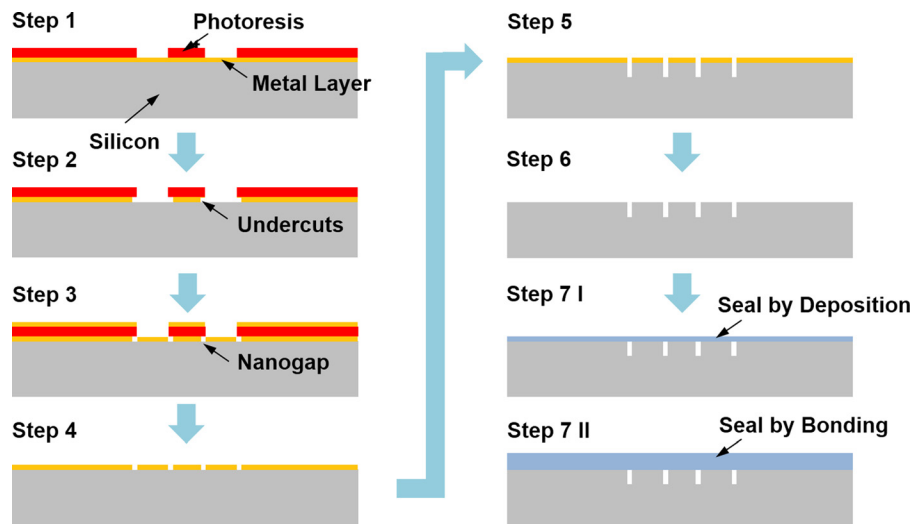
FIG. 8. Schematic of nanochannel fabrication based on edge lithography technique. Step 1: Deposition and patterning of the first metal layer. Step 2: Formation of undercuts using isotropic etching. Step 3: Deposition of the second metal layer. Step 4: Photoresist lift-off. Step 5: Formation of open nanochannels using DRIE. Step 6: Removal of the metal mask. Step 7: Nanochannel sealing using deposition (7 I) or bonding (7 II).

growing another material onto the trenches after removal of the metal mask.[165] For silicon substrates, this can be done by controlled thermal oxidization. Xie *et al*. have used this method to further shrink the channel width and produced wafer-scale 2-D high-AR vertical nanochannels.[167]

Another approach that employs controlled etching to fabricate vertical nanochannels is based on spacer technique.[168] In this approach, the nanoscale width of the nanochannels is defined by the thickness of the spacer layer.[169–171] The process is schematically illustrated in Figure 9. As the first step, a standard photolithography is used and followed by anisotropically etching the substrate to form vertical trenches with micrometer sized openings. The height of these vertical trenches determines the final height of the nanochannels. Afterwards, a thin spacer layer is uniformly deposited on the substrate using CVD technique (step 2). Vertical anisotropic etching is then performed again on the substrate (step 3). This etching step removes all the deposited spacer materials except those at the sidewalls of the trenches, which will serve as the male form of the vertical nanochannel. Subsequently, a thick capping layer is deposited on the substrate to cover the sidewall spacer and fill out the vertical trenches (step 4). Chemical-mechanical-polishing (CMP) is then used to planarize the surface until the sidewall spacer layer is exposed again (step 5). Finally, a selective etching step is applied to remove the spacer to form open vertical nanochannels.

These nanochannels can be used as vertical nanochannel membrane directly (step 6I). Smith *et al*. fabricated such membrane structures with nanochannel feature width of 5–100 nm and used them to separate endotoxin from deionized water.[169] They can also be sealed by bonding or deposition techniques for other lab-on-a-chip applications (step 6II). Lee *et al*. used evaporated gold layer and PECVD silicon oxide to create sealed vertical nanochannels with feature width down to 25 nm.[170] It is worth noting that CMP is not a required step to ultimately remove the spacer layer. In fact, sacrificial layer releasing can be implemented as an alternative to form seal nanochannels once the capping layer is deposited (step 6III). Tas *et al*. fabricated 1-D nanochannels that are 40 nm in width and 90 nm in height using this method.[171]

There is no doubt that fabrication approaches based on edge-lithography and spacer techniques provide new methods to create 2-D vertical nanochannel structures, which otherwise could only be formed by expensive nanolithography based approaches (e.g., EBL and NIL) before. However, these two approaches still cannot completely replace nanolithography based approaches as the density of the nanochannels, determined by the space between nanochannels, is still limited by optical lithography.
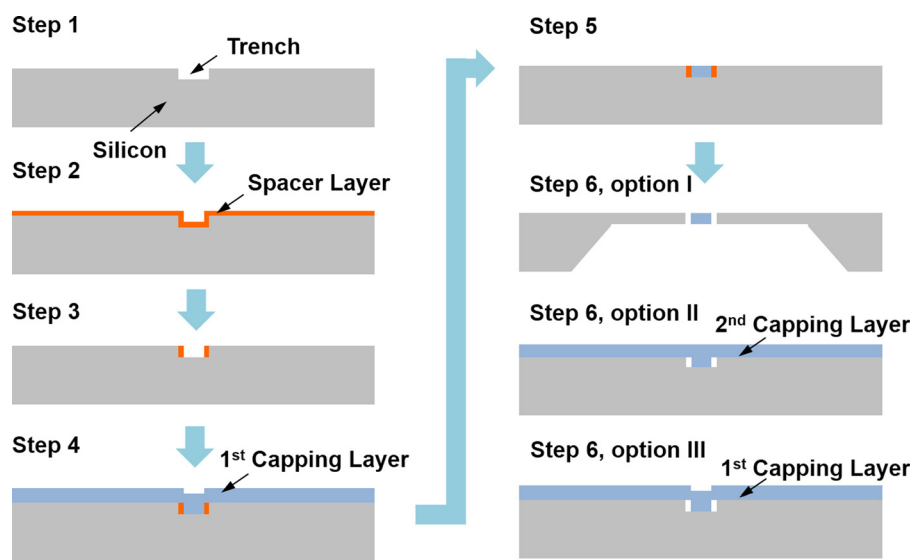
FIG. 9. Schematic of nanochannel fabrication based on spacer technique. Step 1: Patterning and etching of vertical trenches with micrometer sized openings. Step 2: Deposition of the spacer layer using CVD technique. Step 3: Vertical anisotropic etching to form the male form of nanochannels. Step 4: Deposition of the capping layer. Step 5: Surface planarization using CMP. Step 6: Nanochannel formation. Option I. Fabrication of nanochannel membrane by selectively etching nanochannels and back reservoir. Option II. Fabrication of sealed nanochannels using etching and bonding/deposition technique. Option III. Fabrication of sealed nanochannel using sacrificial layer etching. Step 5 is not required in this process.

IV. NANOMATERIAL BASED NANOFABRICATION APPROACHES

With the rapid development of nanotechnology, a variety of chemical substances or materials, so-called nanomaterials, with morphological feature size at nanoscale have been synthesized or manufactured. Recently, using these nanomaterials to prepare nanofluidic devices has become a popular fabrication strategy. Various nanomaterials, from molecular-scale porous ion selective polymers to nanoporous membranes, and from 0-D nanoparticles to 1-D nanowire and nanotube, have been used to prepare nanofluidic devices by taking advantages of their essential nanometer-size features. This section will review recent achievements in the preparation of nanofluidic devices based on this idea.

A. Ion selective polymer

Ion selective polymers are chemical substances having a network shaped backbone with fixed ionic groups tailored and molecule-sized pores inside. When in contact with electrolytes, these ionic groups will attract counter ions, but repel co-ions from entering this nanoporous structure as a result of electrostatic interaction in the nanoscale confinement. Although their regular application is focused on large-scale water pretreatment in a form of membrane, ion selective polymers are now expanding to construct nanofluidic devices by different patterning approaches.

The most straightforward patterning method to prepare nanofluidic devices with ion selective material is based on traditional contact photolithography. For example, through sequential lithography and etching processes, cation-selective polymer, over-oxidized poly(3,4-ethylenedioxythiophene) poly(styrenesulfonate) (PEDOT:PSS), and anion selective material, quaternized and cross-linked poly(vinylbenzylchloride) (PVBC), were integrated into a single device to realize ion bipolar junction transistors and chemical logic gates.[172,173] This contact lithography patterning approach can guarantee a high resolution but requires the ion selective polymers being of solid and compatible with chemicals used. Alternatively, lithography can be applied on prepolymer to realize patterns of certain ion selective polymers when they are UV-curable essentially or become UV-curable with additive photoinitiators. However, this approach faces a

serious contamination issue caused by the possible adhesion between the un-cured prepolymer and the mask during contacts in traditional lithography. Several non-contact lithographic strategies have been advanced to address this problem. For instance, poly (2-acrylamido-2-methyl-1-propanesulfonic acid) (PAMPS), a positively charge selective hydrogel, was polymerized *in situ* by an optofluidic maskless lithography system to form a cation-selective filter between two microchannels for sample preconcentration.[174] Similarly, heterogeneous nanoporous junctions were achieved by patterning cation-selective hydrogel precursors, such as 2-hydroxyethyl methacrylate-acrylic acid (HEMA-AA)[175] or AMPS,[176] and anion selective ones, like 2-(dimethylamino)-ethyl methacrylate (DMAEMA)[175] or (diallyldimethylammonium chloride) DADMAX[176] in a non-contact lithographic platform with the help of corresponding photoinitiators. Microfluidic patterning approach has also been used to pattern ion selective polymer by filling the ion-selective resin in a tentative PDMS microfluidic channel. After drying the resin for 12 h under ambient conditions and removing the PDMS channel, ion-selective microelectrodes were prepared for electrochemical activation and inhibition of neuromuscular systems.[177] Although these non-contact lithography techniques can partially solve the contamination issue that traditional photolithography faces during patterning prepolymers, their spatial resolutions are still limited, which may block their application in the future large-scale integration of micro/nanofluidics.

Among all the ion selective polymers used in nanofluidics, Nafion, a sulfonated tetrafluoroethylene-based fluoropolymer-copolymer discovered by DuPont in the late 1960s, is the mostly used and commercially available proton-selective material. This material has been extensively used in fuel cell,[178] sea water desalinization,[15] and highly selective nanofluidic ion channels. To fabricate a nafion based nanofluidic device, a facile approach is infiltrating resin-type nafion between gaps created by mechanically cutting the PDMS substrate.[15,179] Another way was patterning a very thin nafion resin layer with thickness of hundred nanometers by either stamping[180,181] or microfluidic patterning[180,182–185] approaches on the substrate. Besides the above two approaches using nafion resin, thin film typed nafion, which is also off-the-shelf, was also manually assembled with PMMA microstructures to generate electroconvection and concentration polarization zone for a high throughput pressure-driven micromixer.[186]

B. Nanoporous material

Nanoporous materials, which have large porosity (usually greater than 0.4) and pore diameter between 1 and 100 nm, have been used to construct nanofluidic devices for both fundamental studies and large-scale applications because of their high surface to volume ratio, ordered and uniform pore structure, versatile and rich surface composition and properties.[187] In this sub-section, we will introduce several nanoporous materials including 1-D nanoporous membrane and 3-D nanoporous matrix, and show how to prepare different nanofluidic devices from these materials.

Anodized aluminum oxide (AAO) is one of the widely used and commercial available 1-D nanoporous membranes. As shown in Figure 10(a), AAO membrane contains a high density of uniform cylindrical pores that are aligned perpendicular to the surface and penetrate the entire thickness of the membrane. AAO is usually formed when aluminum is electrochemically oxidized (anodized) in certain solutions.[191] Alumina, the material of AAO, is positively charged when in contact with aqueous solution and is ready for biomolecule adsorption[192] or chemical modification.[193–195] Because of the unique nanoscale structure and surface property, AAO is very suitable for high throughput nanofluidic applications, such as low-voltage electroosmosis pump,[188,196,197] thin film interference spectroscopy sensing,[196] protein filtering,[195,198] DNA sensing,[193,194] and large-scale gate-all-around nanofluidic field effect transistors.[199] Generally, AAO membrane used in the nanofluidic study has nanopore diameter of ten nanometers or larger, and membrane thickness of micrometers. To further reduce the opening pore size, controlled grazing angle Ar+ ion milling has been applied to sculpture the U-shaped bottom, which is usually formed in the so-prepared AAO nanochannels, and obtained the pore aperture down to 10 nm or below.[200] Very recently, by finely controlling the anodization process, AAO templates with sub-10 nm pore diameters have been successfully prepared.[201] Besides the pore size,
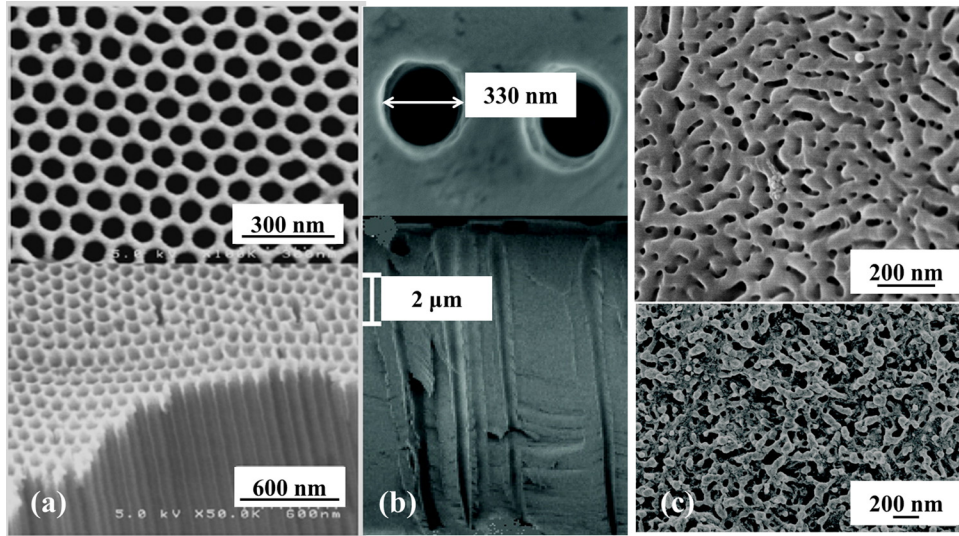
FIG. 10. Typical SEM photos of various nanoporous materials, top: top-view; bottom: cross-sectional view. (a) AAO membrane. Reprinted with permission from Vajandar *et al.*, Nanotechnology **18**(27), 275705 (2007). Copyright 2007 Institute of Physics. (b) Track etched nanoporous membrane. Reprinted with permission from Ali *et al.*, ACS Nano **3**3, 603–608 (2009). Copyright 2009 American Chemical Society. (c) BCP nanoporous matrix. Reprinted with permission from Uehara *et al.*, ACS Nano **3**4, 924-932 (2009). Copyright 2009 American Chemical Society.

distribution of nanopores in AAO can also be tuned by controlled anodization after introducing pre-defined nanopatterns by EBL,[202] FIB direct writing,[203,204] or FIB lithography[205] at the very beginning. Moreover, nanochannels in an AAO membrane can be selectively closed and reopened by tuning the FIB beam energy from 30 keV to 5 keV,[206,207] which is able to isolate individual nanochannel for quantitative nanofluidic study.

Track etched nanoporous membrane, shown in Figure 8(b), is another widely used 1-D nanoporous membrane in nanofluidics. This material is usually prepared in a polymer membrane by chemically etching the damage trails caused by heavy ion radiation.[208–211] Briefly, single swift heavy ion beams (MeV per nucleon) from accelerators generate latent tracks through polymer membrane. A corresponding chemical etching, either one-side etching with the help of electrostopping technique[212] or surfactant-assisted etching,[213] removes the damage zone of the latent tracks and leaves hollow structures through the membrane. The resulting nanopores can be either funnel, bullet, or cone-shaped by tuning radiation ion source, substrate polymer, etching method and condition.[214] They have been demonstrated in both array and single nanopore forms in three different polymer membranes including PC,[215–219] polyethylene terephthalate (PET),[17,189,209,220–227] and polyimide (PI).[214,228,229] Each of these three track etched membranes has its own advantages. PC membranes with track etched sub-10 nm in diameter nanopores are commercially available right now and have been used for separation purpose.[217] Nanopores fabricated in PET foil exhibit a high surface charge density as well as excellent surface modification ability,[220,223] which make them a good model for asymmetric electrokinetics study such as nonlinear ionic current rectification[220,222] and oscillations.[17] Because of the good chemical stability of polyimide, track-etched nanopores in polyimide usually have a constant ionic current readout in various electrolytes, which have been used for bio-sensing[225,228] and ionic device[230] applications.

In addition to the above two 1-D nanoporous materials, 3-D nanoporous matrix prepared by a so-called block-copolymer (BCP) approach has also been reported (Figure 10(c)).[231] For example, by selectively removing the amorphous phases in the crystallized polyethylene/polystyrene (PS) di-block copolymer, a nanoporous membrane with thickness of several micrometers and pore size controllable from 5 to 30 nm was prepared.[190] Surface properties of nanopores prepared by this chemical approach can be precisely tuned, which is important for further

biological/chemical functionalization. For example, block copolymer with terminal of di-COOH group was used to prepare nanoporous membrane for the discrimination of DNA targets with a single-base mismatch.[232] Presently, the biggest concern of applying BCP in quantitative nano-fluidic study is its irregular pore shape, as shown in Figure 10(c).

Overall, nanoporous materials provide excellent nanoscale confinement, but assembling them with microstructures to form an applicable nanofluidic device relies on heavy manual operations, which are time-consuming, non-compatible with traditional MEMS technique, and difficult in establishing an integrated multi-functional micro/nanofluidics. Recently, it has been explored by *in situ* anodizing and etching aluminum film deposited on top of a silicon wafer, which will definitely expand the applications of AAO in more powerful integrated micro/nanofluidics.[198,233,234] A facile and MEMS compatible process was also developed to prepare nanoporous structure by involving a solvent-extraction process in the lithography of a regular photoresist, such as SU-8,[235] which may open a new strategy for applying nanoporous materials in Nanofluidics study.

C. Nanoparticle crystal

Thanks to the rapid development of nanoparticle synthesis in the past decades, monodispersed nanometer-sized particles with various surface functional groups have been commercially available. Self-assembly of nanoparticles into well-organized nanostructures, usually called as nanoparticle crystal, photonic crystal, or synthetic opal as well,[236] has been considered as a valid structured nanomaterial preparation method for different applications including photonic information[237] and Bragg diffraction based biological/chemical sensors.[238] Nanoparticle crystal can also be used as a template to replicate the long-ranged ordered structure into another solid matrix, called as inversed opal, by filling the interstices and then releasing the particles.[239] Other than its original optical applications, nanoparticle crystal has recently been proposed as a nanoporous matrix for various electrophoresis separations[240–242] and sensing[243] by utilizing the steric effects. More interestingly, Chen *et al*. demonstrated for the first time that interstices in a self-assembled nanoparticle crystal formed a three dimensional nanochannel network in a FCC form which had the same electrokinetic property as a single nanochannel but with an enlarged electrical readout.[244] This presented a new perspective on nanoparticle crystal's application in nanofluidics. In a simple analogy to a nanotube, the equivalent diameter of the 3-D nanoscale interstice confined by neighbored nanoparticles can be estimated as 23.38% of the packed particle diameter.[244] To form a nanoparticle crystal in a microchannel, an evaporation-assisted strategy has been reported, as shown in Figure 11. The evaporation induced self-assembly[240,244] starts with loading nanoparticle suspension, usually nanoparticles in water or ethanol, into one reservoir of the microchannel, as shown in steps 1 and 2. Surface tension then drives the
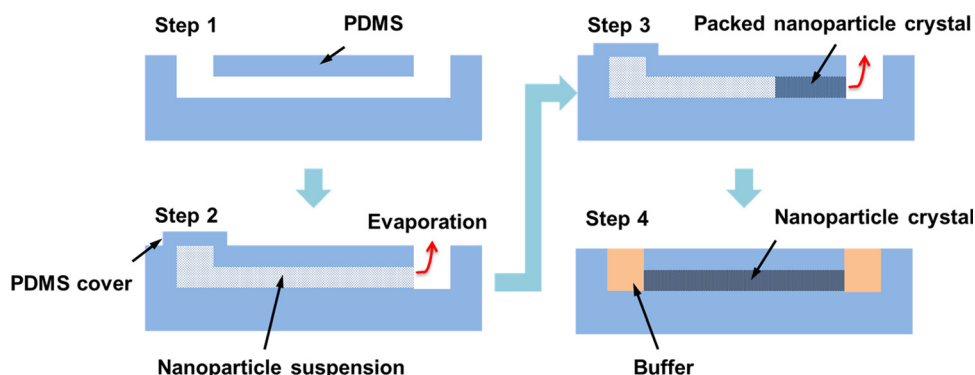

FIG. 11. Schematic of nanofluidic devices fabricated by self-assembling nanoparticles. Step 1: Fabrication of microchannels with reservoirs on both ends. Step 2: Introduction of nanoparticle suspension from one reservoir. Step 3: Self-assembly of nanoparticle crystal based on capillary evaporation. Step 4: Removal of extra nanoparticles by exchanging the buffer solution.

meniscus moving forwards until the meniscus stops at the connection between the microchannel and another reservoir due to the sudden-expansion of the flow duct, as indicated in step 3, exactly the principle of a capillary valve.[245] Without extra input power, the meniscus tends to keep its shape and position. The continuous evaporation of solvent then leaves nanoparticles packed from the meniscus. During this process, the inlet is usually covered by a PDMS sheet to prevent evaporation. The assembly process can be stopped by replacing the nanoparticle suspension in the inlet with suitable buffer solution. Finally, buffers are loaded into two reservoirs for corresponding nanofluidic study, shown in step 4. Recently, some novel approaches have reported to pack nanoparticles into designed patterns using PDMS stamping[246] or inkjet printing,[247] which can further explore the applications of nanoparticle crystal in the nanofluidics study.

Nanofluidic devices made by this nanoparticle packing approach can easily change surface properties by modifying or replacing the nanoparticles, showing promise in electrokinetics-based biosensing applications and fundamental studies. As a proof-of-concept experiment, Lei *et al.* reported an nM-level biotin detection by assembling streptavidin modified nanoparticles (540 nm) in a suspended micropore.[248] By packing nanoparticles with different surface charges[249] or diameters[250] in a suspended micropore structure sequentially, nanofluidic diodes were achieved. Another typical nanofluidic electrokinetic phenomenon, ion concentration polarization, was also realized by self-assembling nanoparticles in a microchannel.[246]

Assembling nanoparticles to construct nanofluidic device has many advantages, such as low cost, simple and fast fabrication process; large effective cross-sectional area, i.e., large electrical readout; and more importantly, mature surface modification methods, which make it easy to graft probes onside for versatile biosensing. It can be foreseen that nanoparticle crystal will get more and more attentions in nanofluidics, especially in its biosensing applications. However, self-assembly nanoparticles in a microstructure still need extra efforts to improve their overall size-controllability and crack-free integrity, which are important for robust sensing performance and high batch-to-batch repeatability. Recently, Zeng *et al.* used multiple evaporation microchannels to avoid the drying-induced cracks during the colloidal crystallization and formed a large scale nanoparticle crystal in microdevice.[242] Meanwhile, electrokinetics of the three-dimensional nanochannel network inside the nanoparticle crystal needs further studies to provide a more precise and fundamental understanding. Using smaller nanoparticles may not be as straightforward as it looks, although it could realize a much smaller feature size and thereby work at a relatively high ionic concentration. Initial wetting of nanoparticle crystal with particle diameter less than 100 nm could be a big issue and will still require reliable solutions.

D. Nanowire and nanotube

Being two widely used 1-D nanomaterials, nanowires and nanotubes have been employed to fabricate different nanochannels for a long history. Nanowire can function as either a template[251] for hot embossing based replication (Figure 12(a)) or a sacrificial master for molding[252–254] (Figure 12(b)) and lithography[255,256] (Figure 12(c)) based nanofabrications. When used as templates, high-hardness nanowires dispersed on a stiff substrate are first embossed into certain polymer (polycarbonate for example), as shown in Figure 12(a) step 1. The polymer replicate is then separated from the nanowires (step 2) and bonded to another substrate with predefined microchannels onside to form the final micro/nanofluidic device (step 3). When used as sacrificial masters, nanowires that can be selectively etched (e.g., silver or zinc oxide,[253] electrospun polyvinylpyrrolidone (PVP),[254] etc.) are usually more preferred. These nanowires can be assembled on top of pre-patterned microstructures to function as masters for various polymer replications, as shown in Figure 12(b) (step 1). After releasing the nanowire along with the microstructures embedded in the replica in corresponding etching baths, polymer micro/nanochannels are obtained, as shown in Figure 12(b) (steps 2, step 3). Alternatively, one can disperse these nanowires on plain substrates first (Figure 12(c), step 1) and then use traditional MEMS techniques including thin film coating/deposition, photolithography and etching to create all related microfluidic components (step 2), and release the nanochannels
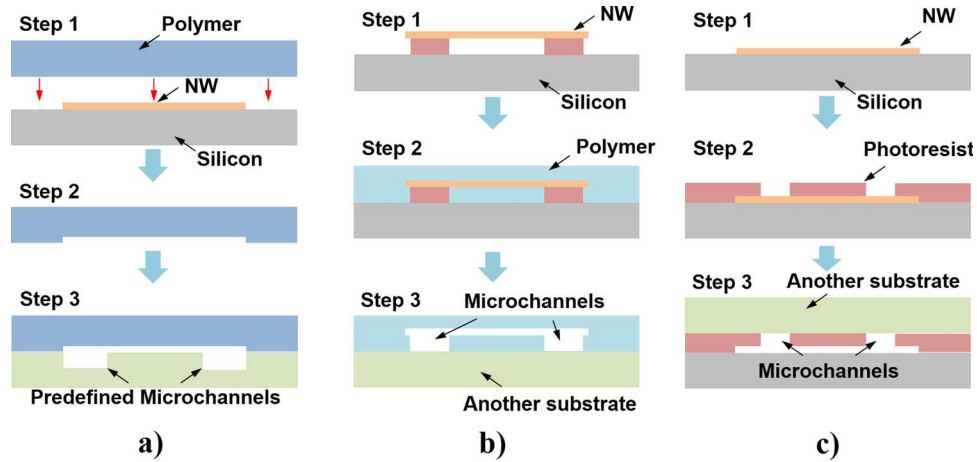
FIG. 12. Schematic of nanochannel fabrication using nanowires. (a) Hot embossing based nanochannel fabrication. Step 1: Hot embossing with nanowire (NW) as master. Step 2: Removing the nanowire. Step 3: Bonding to substrate with predefined microchannels; (b) molding based nanochannel fabrication. Step 1: Assembling nanowire onto microstructures. Step 2: Casting polymer. Step 3: Releasing/removing the nanowire and microstructures and bonding with another substrate; and (c) lithography based nanochannel fabrication. Step 1: Assembling nanowire on the wafer. Step 2: Patterning photoresist. Step 3: Releasing nanowire and bonding with another substrate.

(step 3). This approach is very similar to the SLR method that we have introduced in Sec. III A. Photoresist[255] or other deposited materials, such as silicon oxide[256] has been used as the capping layer. Usually, nanowire based nanofabrication presents circular cross-sectional channels for nanofluidics applications. Nevertheless, some synthesized nanowires presented an ortho-hexagonal cross section, which can thereby be used to fabricate non-circular nanochannel.[255] In addition, electrospinned polymer nanofibers are used to prepare nanofluidic channel with an elliptical cross section[188] or a U-shaped cross-section.[257]

Compared with nanowires, varied nanotubes have been directly used as nanofluidic channels by assembling them within a membrane[258,259] (Figure 13(a)) or bridging them between two microchannels[260–263] (Figure 13(b)). Hinds *et al.* first reported a nanoporous membrane
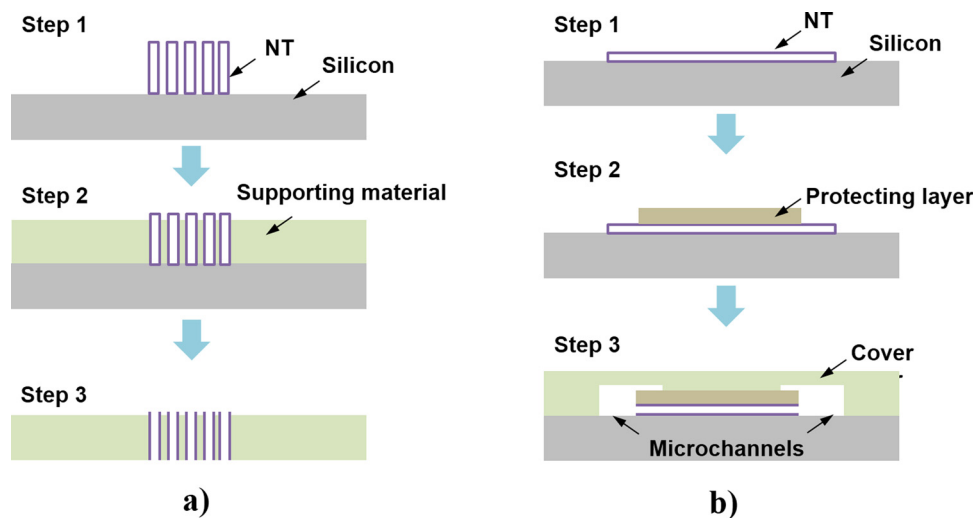
FIG. 13. Schematic of nanochannel fabrication using nanotubes. (a) Suspended nanotube membrane. Step 1: Growing nanotubes (NTs). Step 2: Filling nanotubes with supporting material. Step 3: Releasing the NTs-embedded polymer membrane and opening the nanotubes; (b) nanotube embedded micro/nanofluidic device. Step 1: Growing nanotube on top of wafer. Step 2: Patterning photoresist or other protecting layer by lithography. Step 3: Opening the nanotube and packaging the structure with another wafer.

fabrication strategy by encapsulating vertically grown carbon nanotube (CNT) array with polymer.[258] Briefly, as shown in Figure 13(a), nanotubes are grown on top of the substrate vertically (step 1), and then filled with corresponding polymer (step 2). After releasing the polymer with nanotubes inside and opening the nanotube ends, a CNT membrane is formed (step 3). Besides CNT, inorganic nanotubes can also be used to form a nanotube-embedded membrane with the help of microfabrication technique.[264] Lithography based patterning on horizontally oriented nanotubes with different protecting materials, such as PMMA resist[262] and silicon oxide,[260,261,263] is another fabrication strategy for inorganic nanotube integrated micro/nanofluidic device, as illustrated in Figure 13(b). Here, nanotubes are grown or dispersed on top of the substrate horizontally (step 1). A protecting layer is deposited and subsequently patterned using photolithography and etching as illustrated in step 2. After packaging the substrate with corresponding material and opening the nanotube ends, a nanotube based micro/nanofluidic device is obtained (step 3). Moreover, nanotube has also been molded to form a nanochannel with a process similar to Figure 12(b) by replacing nanowire with corresponding CNT.[265] More recently, fluid flow inside nanotube was experimentally measured by directly loading water into CNT without any capping or protection layer.[266] Details on nanotube-based nanofluidic study can be found in some excellent reviews.[267,268]

Owing to the rapid development of synthesis techniques of 1-D nanomaterials, using nanowire or nanotube to construct nanofluidic device is relatively simple and, in a sense, low-cost. This strategy is capable of fabricating 1-D nanochannels with uniform surface properties and feature size ranging from sub-1 nm[266] to several tens of nanometer or even larger. It can also form heteostructured 1-D nanochannels with distinctive surface properties along the channel. For example, a longitudinal heterostructured SiO_2/Al_2O_3 nanotube was prepared for ionic current rectification study.[261] Currently, alignment between nanowire/nanotube and microstructures is the most challenge issue in this nanofluidic device fabrication strategy. Several alignment methods have been reported, such as using direct mechanical manipulation,[251,255] dielectrophoresis arrangement,[265] random dispersion,[253,259,262] and directional *in situ* electrospinning[188,254] or growth.[260,261,263,266] However, none of them can be as robust and high throughput as the traditional maker-based optical alignment. For CNT-based nanofluidic devices, there is another fabrication issue regarding opening the tube end for sample loading. Oxygen plasma etching is the major method[262,263,265] but this method is lacking of precise control and may overetch CNTs. Recently, it has been reported that electrical breakdown of carbon nanotube under water droplet was able to open the tube *in situ* for fluid flow experiments,[266] which may present a new choice to prepare compact and controllable CNT nanofluidic devices.

V. OTHER METHODS

In addition to the above three main nanofabrication strategies, some interesting chemical properties, physical phenomena, and biological structures have been harnessed to construct nanofluidic devices. Although these unconventional approaches usually fail to present a reliable controllability on channel geometry and size, they do provide alternative solutions for the preparation of nanofluidic devices and, in most cases, are even simpler and cheaper than nanofabrication methods we introduced above.

Organic polymers are unstable to UV exposure, easy to crack under stress and deform with loads. These properties can be utilized to create nanochannel-shaped structures for nanofluidic devices. It has been reported that certain polymers, including PC[269,270] and PMMA,[271] decompose upon UV exposure and leave nanoscale structures on the surface. This phenomenon has been developed as a new sculpturing method to produce 1-D nanochannels. Meanwhile, stress-mismatch-induced nanometer-sized cracks on some polymers surface, such as PDMS[272,273] and PS,[274] formed by mechanical stretching or thermal annealing have been proposed to function as nanochannels. These nanoscale cracks can be as small as 20 nm in depth[274] and are able to connect with microchannels to form integrated micro/nanofluidic devices.[273] Similar cracks were also found in printed toners after being electrically broken down and were used to bridge two microchannels for nanofluidics based protein preconcentration.[275] Moreover, nanochannel

structures can be created based on polymer deformation. Taking advantages of the excellent thermal plasticity property of PMMA, nanochannels with width down to 132 nm and depth of 85 nm were formed by shrinking pre-prepared PMMA microchannels in a thermal compression process.[276]

Besides utilizing special properties of polymers, in certain conditions, failures in traditional microfabrication can be converted as new methods for nanochannel fabrication. One of the examples is interstices of polycrystalline grains formed inside thin films during a controlled CVD[277,278] or PVD.[279] These interstices usually at sub-10 nm scale have been used as nano-sieves for protein separation. Another example is nanoscale fractures on fused silica microtube generated around a scratch either by manually pushing the scratch point or using a supersonic probe. Nanofractures with feature sizes from 11 nm to 250 nm were formed by this method and used for DNA preconcentration.[280] In addition to these two cases, bonding failures during PDMS-glass bonding have been explored. It has been reported that insufficient bonding between plain PDMS and glass substrates may leave nanometer-sized gaps that can be successfully utilized for protein preconcentration.[281,282] It has also been shown that the so called "roof collapse" of PDMS deformation during bonding of PDMS microchannels with large width to depth ratio (small AR) can generate triangular-shaped nanochannels with feature size around hundred nanometers at the edge.[283] Similar nanochannels were also formed by replicating protein deposit from confined solution evaporation in deformed PDMS microchannels.[284]

As another nanochannel preparation strategy, more recently, traditional microscale, or even macroscale, machining techniques have been expanded to achieve nanoscale structures. It is well known that glass or quartz capillaries can be pulled with a laser-equipped pipet puller into microcapillaries. This technique has been improved to realize nanometer-sized capillaries with the feature size down to 45 nm.[285] Coincidentally, materials processing with femtosecond laser pulses, a widely used micromachining method in optics, has been modified to ablate metal thin film to form nanochannels with feature size of hundred nanometers.[286] Besides these micromachining methods, injection molding technique for mass production of disposable all-polymer devices in traditional machining industry has been optimized to demonstrate an ability in fabrication of nanochannels with width down to 140 nm and depth of 150 nm.[287]

In addition to the above attempts, nanofluidic devices, nanopores in particular, can also be realized by utilizing pore-forming proteins. These mushroom or cylinder shaped protein molecules have a nanometer-sized hollow core and thus can be used as nanopores directly after being inserted in a lipid bilayer membrane. The most widely used pore-forming protein is α-Hemolysin, a monomeric, 33 kD, 293-residue protein that is secreted by the human pathogen *Staphylococcus aureus*.[288] α-Hemolysin can be modeled as a nanotube with 10 nm in length and 1.4–4.6 nm in diameter[289] and has found great potential in single biomolecule detection and analysis, including DNA/RNA sequencing,[290] protein/microRNA detection,[291–293] and kinetic studies.[294] Beyond α-Hemolysin, several other proteins, including OmpF[295] and MspA[296] porins have also been investigated as nanopores for similar applications. Recently, ringlike Stable Protein 1 and its derivatives have been assembled to form hydrophilic nanochannels in the plasma membrane of living cells and ohmically link the cell interior and the electrical sensing pads for neuroelectronic study.[297] All these protein-based nanopores/nanochannels mentioned above, along with other pore/channel forming proteins[298] have well-defined nanoscale confinement and excellent reproducibility. However, compared with solid state counterparts, they cannot be designed at will, and lack durability due to the fragile nature of the supporting lipid bilayers.

VI. MATERIAL AND FABRICATION GUIDELINES

Tables I–III list all fabrication approaches in this review and compare them in terms of geometrical characteristics, manufacturing features, process compatibility, and materials. As shown in these tables, in general, nanolithography based fabrication approaches exhibit high resolutions and excellent compatibilities with traditional microfabrication processes. However, these approaches usually require a high investment for the fabrication facility along with an

TABLE I. Comparison of nanolithography-based nanofabrication methods (Sec. II).

		EBL (II A)	FIB (II B)	NIL (II C)	IL (II D)	SL (II E)
Geometrical characteristics	Feature size[a]	Sub 10 nm or larger	Around 10 nm or larger	20 nm or larger	25 nm or larger	Around 10 nm or larger
	Size controllability	Excellent	Excellent	Excellent	Excellent	Good
	Dimension	1D/2D (vertical)	0D/1D	1D/2D (vertical)	1D/2D (vertical)	0D
	Shape and form	Rectangular cross-section; single channel or small scale channel array	Shape controllable pore or V-shaped channel; single channel, small scale pore/channel array	Large scale channel array	Large scale channel/pore array	Circular nanopore Ordered nanopore array
Manufacturing cost[b]	Running cost	High	High	High, Medium for repeated use	Medium	Medium
	Facility	EBL system, MEMS (RIE)	FIB system, MEMS (processes to prepare the membrane)	NIL system, MEMS (RIE)	IL arrangement (interferometer) MEMS (RIE)	MEMS (processes to prepare the membrane), monolayer nanoparticle facility
	Time	Medium	Short	Medium	Medium	Medium
Process compatibility[c]	MEMS techniques	Yes	Post	Yes	Yes	Yes, but not yet wafer-scale
	Soft-lithography techniques	Master, Pre-	Master, Pre-	Master, Pre-	Master, Pre-	Pre-
	Material of substrate	Varies, usually silicon based materials	Varies, usually silicon based materials	Varies, usually silicon based materials	Varies, usually silicon based materials	Varies, usually silicon based materials

[a]Feature size refers to the characteristic size obtained directly by the corresponding approach. Additional size tuning or shrinking operations are not included.

[b]Here, only the steps that create nanoscale features by the corresponding approaches are considered. Other operations, such as fabrications of microchannels/reservoirs and cover sealing, are not included. MEMS facility indicates regular instruments in a MEMS cleanroom for lithography, RIE, DRIE, PVD, CVD, and other MEMS processes.

[c]Compatibility refers to the integration ability of the corresponding approach with traditional MEMS or soft-lithography (PDMS) fabrication techniques. "Post-" means the nanofabrication approach can be operated after MEMS/PDMS operations. In soft-lithography compatibility column, "pre-" indicates that the corresponding approach can be used to prepare nanochannels on a flat surface or nanopore array in a suspended membrane, which then can be bonded with PDMS replicate (with/without microchannels); while "master" means this approach can be used to fabricate the master for soft-lithography.

TABLE II. Comparison of MEMS-based nanofabrication methods (Sec. III).

		Sacrificial layer etching (III A)	Etching and bonding (III B)	Etching and deposition (III C)	Edge lithography and spacer technique (III D)
Geometrical characteristics	Feature size[a]	Around 5 nm or larger	Around 2 nm or larger	30 nm or larger	Around 10 nm or larger
	Size controllability	Excellent	Excellent	Good	Good
	Dimension	1D/2D	2D	2D	2D
	Shape and form	Rectangular cross-section; single channel or small scale channel (low aspect ratio) array	Rectangular cross-section; single channel or small scale channel (low aspect ratio) array	Single channel or small scale channel (high aspect ratio) array	Single channel or small scale channel (high aspect ratio) array
Manufacturing cost[b]	Running cost	Low	Low	Medium	Medium
	Facility	MEMS	MEMS	MEMS	MEMS
	Time	Long	Short	Long	Long
Process compatibility[c]	MEMS techniques	Yes	Yes	Yes	Yes
	Soft-lithography techniques	Pre-	No	Pre-	Pre-
Material of substrate		Varies, usually silicon based materials	Varies, usually silicon based materials	Parylene C, polysilicon, SiO_2	Varies, usually silicon based materials

[a]Feature size refers to the characteristic size obtained directly by the corresponding approach. Additional size tuning or shrinking operations are not included.

[b]Here, only the steps that create nanoscale features by the corresponding approaches are considered. Other operations, such as fabrications of microchannels/reservoirs and cover sealing, are not included. MEMS facility indicates regular instruments in a MEMS cleanroom for lithography, RIE, DRIE, PVD, CVD, and other MEMS processes.

[c]Compatibility refers to the integration ability of the corresponding approach with traditional MEMS or soft-lithography (PDMS) fabrication techniques. "Post-" means the nanofabrication approach can be operated after MEMS/PDMS operations. In soft-lithography compatibility column, "pre-" indicates that the corresponding approach can be used to prepare nanochannels on a flat surface or nanopore array in a suspended membrane, which then can be bonded with PDMS replicate (with/without microchannels); while "master" means this approach can be used to fabricate the master for soft-lithography.

TABLE III. Comparison of nanomaterial-based nanofabrication methods (Sec. IV).

		Ion selective polymer (IV A)	AAO (IV B)	track etched nanopore (IV B)	Block-copolymer (IV B)	Nanoparticle crystal (IV C)	Nanowire (IV D)	Nanotube (IV D)
Geometrical characteristics	Feature size[a]	Sub-nanometer to several nanometers	Sub 10 nm to hundreds nanometers	Sub 10 nm or larger	Around 5 nm–20 nm	Around 10 nm or larger	Several tens or larger	Sub-nanometer to 2 nm (CNT) or larger (inorganic nanotube)
	Size controllability	Low	Low	Low	Low	Medium	Good	Good
	Dimension	0D	0D/1D	0D/1D	0D	0D	1D	1D
	Shape and form	Random shape; bulk nanoporous structure	Random shape (ordered after special pre-definition); single nanopore or nanopore array	funnel, bullet or cone-shaped channel profile with circular cross-section; single nanopore or nanopore array	Random shape; bulk nanoporous material	3D connected nanopore network with a typical periodic structure	Circular-cross section or some other shapes	Single circular-cross sectional nanochannel or nanochannel/ nanopore array
Manufacturing cost[b]	Running cost	Low, off-shelf products available	Low, off-shelf products available	Low, off-shelf products available	Low	Low, off-shelf products available	High	High
	Facility	Chemical bench	Chemical bench	Radiation source	Chemical bench	Chemical bench	Nanowire facility	Nanotube facility
	Time	Short	Short	Short	Short	Short	Short	Short
Process compatibility[c]	MEMS techniques	Yes	Yes	No	No	Post-	Yes, but not yet wafer-scale	Yes, but not yet wafer-scale
	Soft-lithography techniques	Post-	No	No	No	Post-	Master,	Pre-
	Material of substrate	Special polymers	Alumina	PET, PC, PI	Co-polymer	Silica, polystyrene	Varies	Varies, usually carbon-based materials

[a]Feature size refers to the characteristic size obtained directly by the corresponding approach. Additional size tuning or shrinking operations are not included.

[b]Here, only the steps that create nanoscale features by the corresponding approaches are considered. Other operations, such as fabrications of microchannels/reservoirs and cover sealing, are not included. MEMS facility indicates regular instruments in a MEMS cleanroom for lithography, RIE, DRIE, PVD, CVD, and other MEMS processes.

[c]Compatibility refers to the integration ability of the corresponding approach with traditional MEMS or soft-lithography (PDMS) fabrication techniques. "Post-" means the nanofabrication approach can be operated after MEMS/PDMS operations. In soft-lithography compatibility column, "pre-" indicates that the corresponding approach can be used to prepare nanochannels on a flat surface or nanopore array in a suspended membrane, which then can be bonded with PDMS replicate (with/without microchannels); while "master" means this approach can be used to fabricate the master for soft-lithography.

expensive running cost. By contrast, with most materials off-the-shelf or easy to be synthesized, nanofabrication with nanomaterials shows advantages of low cost, fast process, and in some cases, even an extraordinary capability of sub-nanometer-sized fabrication. Nevertheless, using nanomaterials still faces problems including fabrication controllability and compatibility with traditional microfabrication techniques, which require further efforts to improve. Compared with these two strategies, MEMS-based approach is incapable of directly defining nanoscale feature, but still can generate various nanofluidic devices and shows the best performance-price ratio by inheriting the great achievement from well-established microfabrication techniques. To determine which approach should be chosen for a particular nanofluidic device, one has to be aware of the application of the device and the corresponding requirements for channel materials, dimension, feature size, etc. In this section, six such requirements are discussed and a comprehensive guideline is provided to assist researchers towards the most appropriate fabrication choice.

A. Material consideration

Material selection does not only play an important role in determining the fabrication cost but is also vital for proper device functioning since it must be compatible with environmental and operating conditions. Different materials can lead to different fabrication processes; whereas sometimes, depending on the application, the fabrication strategy reversely limits material selection. So far, a wide range of different materials have been employed in the fabrication of nanofluidic device, including silicon based materials (silicon, quartz, glass, and various oxide/nitride), polymers, and sp2 carbon materials.

Among these materials, silicon, quartz, and glass are the major choices of device substrates. Silicon is known as one of the cheapest substrate materials that can be processed by many mature bulk and surface micromachining techniques. Nanochannels fabricated on silicon can be easily integrated with other fluidic components and electric circuits, resulting in fully functional lab-on-a-chip devices. Despite these advantages, silicon is still not an ideal material for nanochannel devices considering the following aspects. It cannot directly serve as nanochannel wall if the application involves any electrokinetic phenomena because silicon is semi-conductive and can lead to noticeable electrical leak. An additional insulation layer such as silicon dioxide and/or silicon nitride is thus required to passivate the nanochannel. More importantly, silicon is not transparent to visible light, and thus may pose a concern for nanofluidics applications with optical observation/operation involved. Compared with silicon, quartz and glass face little insulation and transparency issues, which make them more attractive as substrates for nanochannel fabrication. However, these two materials are generally harder to process. For example, it is very difficult to form deep microchannels/reservoirs with high AR in these two substrates, posing certain challenges for sample introduction and device integration. Moreover, fabrication based on glass substrates needs to avoid high temperature processes (e.g., LPCVD) as glass tends to deform above 400 °C. In addition, glass has a trend to slowly dissolve in aqueous solution.[10] If long-term reliability is a major concern for a particular application, glass may not be an appropriate substrate.

Besides consideration of substrates, material selection for the channel wall is equally important. Currently, most nanochannel walls are made of various oxide/nitride such as silicon dioxide, silicon nitride, and aluminum oxide. These materials ensure an electrical insulating interface and also provide certain amount of surface charges when in contact with aqueous solutions due to surface group dissociation and/or ion adsorption.[299] For example, silicon dioxide is negatively charged while aluminum oxide gives positive surface charges in most aqueous buffer solutions with pH value of 7. These surface charges lead to a surface-charge-governed ion transport phenomenon in nanochannels, which has great potentials in many bio- and energy-related applications. Furthermore, oxide/nitride materials can be modified through various silane chemistries to exhibit tunable surface properties, such as surface roughness, hydrophobicity, charge density, and biological probe.[5,193,300]

In addition to the above inorganic materials, polymers have also served as fabrication materials for nanofluidic device, although not as widely used as those for microfluidics. Polymers,

such as PDMS, PMMA, PET, PC, etc., are promising due to their low cost, high biocompatibility, and optical transparency. By certain chemical treatments, the surface of these organic materials can also exhibit rich surface charges and/or specific functional groups for diverse applications in nanofluidics. However, polymers often exhibit low Young's modulus and low interfacial free energy, which actually become major concerns for their usage in preparing nanofluidic devices due to stress or affinity induced channel collapse and/or unstable surface properties (hydrophobicity recovery). At this point, polymers are mostly used to prepare high AR nanochannels or low AR ones with depth larger than 100 nm.[301]

An emerging new material for nanofluidics is sp2 carbon material, including CNT and graphite. As far as we know, sp2 carbon materials are the only ones that can form atomically smooth hydrophobic surface. Combined with nanoscale confinement, these sp2 carbon materials can significantly enhance fluid transport in nanochannels as they release the non-slip boundary constraint and provide an efficient hopping transport mechanism by forming 1-D water chains. It has been reported that water transport in Single-Walled Carbon Nanotubes (SWCNTs) exhibited an enhancement of three orders of magnitude over continuum hydrodynamics models.[16] Surface properties of sp2 carbon materials can also be tuned with various chemical treatments to meet the requirement raised by nanofluidics applications.[302–304] Current developments of these materials are hampered by difficulties in manipulation and assembly. Although CNT based nanochannel devices have been fabricated (see Sec. IV D), these devices are still facing challenges in integrating with other fluidic components and thus hardly find applications in lab-on-a-chip.

B. Geometry consideration

Geometry, including dimension, size, and uniformity, is another important factor that will determine the fabrication strategy for target nanofluidic devices. Figure 14 shows the typical channel-width/channel-height (depth) that can be reached by the main fabrication approaches summarized in this review, which is helpful to guide corresponding fabrication process design.

1. Dimension (aspect ratio)

Generally speaking, the desired application of a particular device determines its dimension and the dimension decides the fabrication approach in turn. As mentioned in the introduction section, typical nanochannels are of three types based on dimensional categories: 0-D, 1-D, and 2-D. These nanochannels can be further classified into two sub-categories based on their forms, i.e., individual nanochannels and nanochannel arrays.

0-D nanochannels, in their array forms, are mainly used to construct membranes for large-scale applications, including sample separation, water purification, energy conversion/storage, drug delivery, and so on.[305] Presently, these nanochannels can only be prepared by nanomaterials, which have been summarized in several sub-sections of Sec. IV. In contrast, individual 0-D nanochannel, usually called nanopore, is preferred for single molecular studies (e.g., DNA sequencing, protein detection, etc.[306,307]) since their cross sectional area is comparable to individual biomolecules and thus can provide good confinement and high sensitivity. Individual 0-D nanopore is mainly formed by FIB or ion-track etching, which has been briefly introduced in Secs. II B and IV B. Interested readers are recommended to check the following excellent reviews[22,308] regarding the fabrication of solid state nanopores. Individual 0-D nanopore can also be obtained by inserting some special proteins (such as α-hemolysine) into lipid membrane, as introduced in Sec. V.

1-D nanochannels usually find similar applications as the 0-D nanochannels,[16,260,262] while they are also good candidates for fundamental transport study[90,266,309] as they usually have more uniform and controlled geometry. The best way to fabricate 1-D nanochannels, either in array or individual form, is bottom–up approaches based on existing 1-D nanomaterials such as nanotubes, nanowires, and mesoporous materials (see Sec. IV D). In fact, carbon or silica nanotubes have been directly used as 1-D nanochannels due to their hollow structure. Top-down approaches are also possible to fabricate 1-D nanochannel structures, either array or individual,

to address corresponding applications. However, the fabrication process usually involves advanced lithography techniques (Sec. II) or tricky steps such as edge lithography (Sec. III D), which is relatively complex and high-cost. Moreover, it is still extremely difficult to fabricate 1-D nanochannels with both height and width less than 5 nm based on these top-down approaches.

2-D planar nanochannels with low AR, usually individually or in a small scale array, are ideal for sample preconcentration[310]/separation,[311] energy/environmental applications,[15] and fundamental fluid transport[90,312] studies as they provide large observation windows and high flow fluxes while maintaining nanoscale confinement. Traditional MEMS techniques based on optical lithography (including sacrificial layer releasing, Sec. III A, and etching-and-bonding technique, Sec. III B) are very suitable to fabricate such nanochannels because the channel length and width are defined by optical lithography with a resolution around 1 μm while the channel height can be as small as 2 nm.[4] The minimum aspect ratio of these nanochannels is around 1:1000, which is limited by several collapsing mechanisms during fabrication and operation, e.g., electrostatic-force-induced collapse in anodic bonding and capillary-force-induced one during liquid introduction or extraction. The later one is actually a common concern for the operation of all 2-D planar nanochannels. 2-D vertical nanochannels with a high AR are usually prepared as a large scale array for high-throughput applications[163] as they occupy the fabrication area most efficiently. These nanochannels can be made based on most nanolithography techniques (EBL, Sec. II A; NIL, Sec. II C; IL, Sec. II D) or several MEMS fabrication techniques, including etching-and-depositing (Sec. III C), edge lithography and spacer technique (Sec. III D). Among these techniques, EBL is definitely the best in terms of minimum channel width and high channel density. However, this technique is relatively expensive and time-consuming. Furthermore, the channel AR is rather limited due to AR dependent transport and the microloading effect during the DRIE process.[313] Compared with EBL, the MEMS based techniques are much more cost and time effective. The achieved channel AR is also much larger by taking advantages of various size shrinkage approaches in MEMS technique. For example, 2-D vertical nanochannel arrays with an AR up to 400 have been formed using the etching and deposition approach.[163]

2. Feature size

Feature size is another very important factor determining the device performance along with the fabrication strategy. It is widely accepted that the unique transport characteristics of nanochannels result from interactions of several intermolecular forces, including steric/hydration forces (0.1–2 nm in range), van der Waals forces (0.1–50 nm in range), and electrostatic forces (1–100 nm in range).[125] The smaller the channel is, the stronger the intermolecular forces are and the more anomalous ion/molecule transport is expected inside the channel. Because applications of nanochannels also strongly rely on their transport properties, channel feature size is thus another key factor when choosing fabrication techniques. Generally speaking, as the feature size decreases, the choices of fabrication approach decrease while the process complexity increases and the production yield drops down. For sub-5 nm nanochannels where all intermolecular forces are strong, the available fabrication approaches are very limited now. Current methods are mainly based on nanomaterials (Sec. IV) and protein nanopore (Sec. V). Several mesoporous nanomaterials (Sec. IV A), such as nafion, have a pore size around 4 nm or smaller and thus could form a membrane with ultra-small pores. The diameter of carbon/silica/B_3N_6 nanotubes ranges from 0.5 nm to several nanometers, enabling the creation of single 1-D nanochannels and membranes (Sec. IV D). Besides these nanomaterials, two MEMS based fabrication approaches, sacrificial layer releasing (Sec. III A) and etching and bonding (Sec. III B) can provide alternative solutions for nanochannels with a feature size between 2 and 5 nm. However, both approaches require precise etching/deposition control down to 1 nm, which is still not trivial to achieve. Compared to sub-5 nm nanochannels, nanochannels with feature size between 5 and 20 nm can still benefit from van der Waals force and electrostatic force, but the range of fabrication choices becomes much wider. In addition to the above approaches, EBL

(Sec. II A), FIB (Sec. II B), NIL (Sec. II C), SL (Sec. II D) as well as edge-lithography and spacer techniques (Sec. III D) have also been widely used to create nanochannels with such confinement. With the help of some size-shrinkage strategies, such as reflowing or post-deposition/oxidization, these approaches are also capable of generating nanochannels with feature size down to sub-5 nm.

Nanochannels with feature size ranging from 20 nm to 100 nm (the upper limit of the nanochannel definition in this review) can mainly harness electrostatic effects but their fabrication choices are the widest and most abundant. Nearly all the fabrication techniques mentioned in this review have the ability to produce such nanochannels. One has to consider other factors, such as channel uniformity, surface properties, and integration ability to determine the best fabrication method.

3. Channel uniformity

Most fundamental transport studies and certain bio-related applications (sensing for example) in nanochannels require high channel uniformity in terms of height/width/surface properties to achieve linear transport behavior for simple data analysis and deep physical understanding. Current 1-D and 2-D nanochannels made by most nanolithography (Sec. II except of FIB technique) and traditional optical lithography techniques (see Sec. III) generally have uniform cross-section along the channel. However, it is worth noting that high AR nanochannels prepared by nanolithography and Bosch-typed DRIE have a scallop-shaped side-wall profile due to the etching-passivation cycles in the etching, which may limit their applications when geometry uniformity is a big concern. In contrast to uniform nanochannels, nanochannels with varied feature size or non-uniform surface property along the channel are harder to fabricate. These nanochannels can result in non-linear transport behaviors and thus have great potential for biomolecule preconcentration, separation as well as transport control. Up to now, there are limited choices to produce nanochannels with desired non-uniformity. Conical shape nanopores
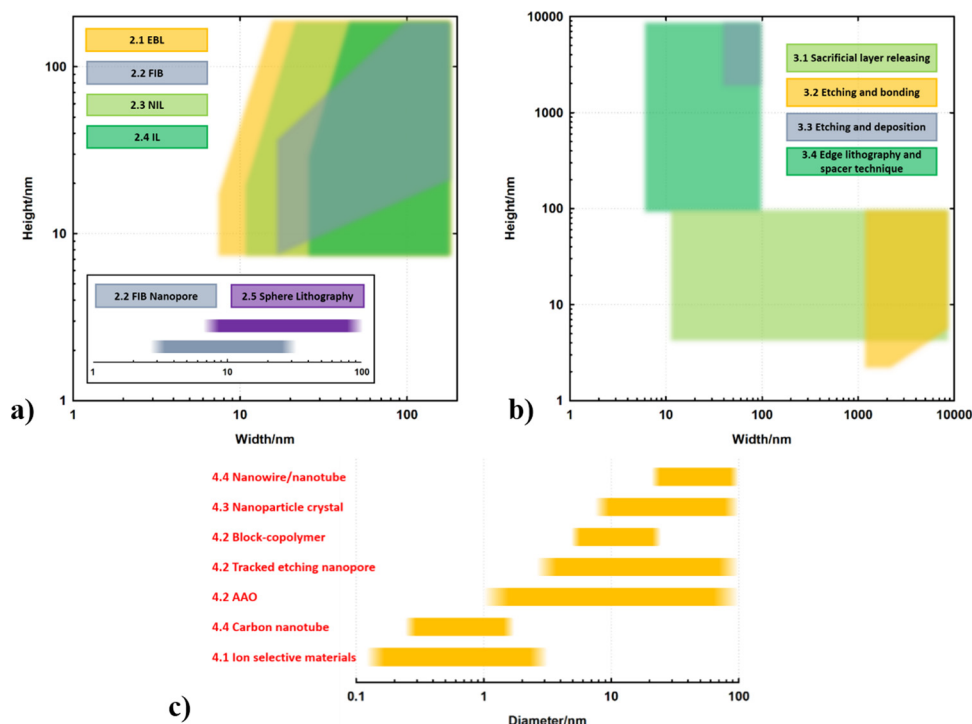

FIG. 14. Achievable geometries and feature sizes of nanofluidic devices using current nanofabrication approaches. (a) Nanolithography based techniques; (b) MEMS based techniques; (c) Nanomaterials based techniques. This figure is based on the authors' understanding of the state-of-the-art of all the nanofabrication approaches in this review.

prepared by FIB (Sec. II B) and track etching (Sec. IV B) are probably the simplest nonlinear nanofluidic devices. Besides nanopores, 1-D/2-D nanochannels with non-uniform channel height can be made by slightly modifying a fabrication scheme of uniform nanochannels. For example, tapered nanochannels can be made during a sacrificial layer releasing process if an etchant with low selectivity is chosen.[4] Recently, a so-called nanoglassblowing technique was developed to fabricate integrated microfluidic and nanofluidic device with gradual depth variation and wide, shallow nanochannels.[314] In addition to these methods for fabricating channels with non-uniform geometry, it is worth mentioning that nanochannel with non-uniform surface properties can be formed by a diffusion-limited patterning (DLP) technique,[5] which provides an alternative solution of introducing non-linear transport behaviors.

C. Other considerations

Besides materials and geometry concerns, one also has to consider other factors, such as integration ability and observation, to determine the best fabrication strategy for a target nanofluidic device.

Nanochannels that are capable of integrating with other fluidic/electronic components are highly desired for micro total analysis systems. As listed in Tables I–III, currently, 1-D or 2-D nanochannels formed by various bulk/surface etching techniques (Secs. II and III, no matter which type of lithography technique is involved) have good integration ability since other functional components can be fabricated on the same substrate. Or, with the help of wafer-level alignment and bonding operations, nanochannel can be integrated with microchannel and reservoirs on different substrates. Compared with these channels, 0-D nanochannels/nanopores and other 1-D nanochannels based on nanomaterials are rather difficult for integration, which restricts their practical applications to some extent.

For studies and applications that involve accurate optical measurements, transparent nanochannels with thin capping layers are preferred since they can lower signal loss, increase image contrast, and reduce the necessities of using long-working distance objective lens. Such nanochannels can be fabricated by sacrificial layer releasing (Sec. III A), etching and deposition (Sec. III C) as well as assembling of 1-D nanomaterials (Sec. IV D). Because the capping layer formed by these techniques can be as thin as several hundred nanometers, these channels can also be integrated with other advanced optical techniques (e.g., whispering gallery mode of optical microcavity, surface enhanced Raman, etc.) for ultra-sensitive optical detection. It is worth noting that among these three techniques, sacrificial layer releasing is the only one that has the ability to fabricate 2-D shallow nanochannels with large optical observation window.

VII. FUTURE PROSPECTS

The past ten years have witnessed the booming development of nanofabrication techniques for nanofluidic devices as summarized above. It is believed with much confidence that in the next ten years, the nanofluidics related studies will remain popular and get fruitful achievements from fundamental understanding of ion and molecule transport at the nanoscale to novel multidisciplinary applications in bio- and energy-related fields. The fast growth of nanofluidics keeps calling for efforts to fabricate nanochannel/nanopore with smaller feature size, to design nanofluidic device with more flexibility in geometry, surface property and function, and in some cases, to prototype the principle device in a more economical and simple way.

Capability of fabricating nanochannels with feature size smaller than 5 nm will definitely take the present nanofluidics study to a whole new level.[2,16,125,262] The confined space with only several tens of layers of molecules existing presents an unprecedented opportunity to explore anomalous fluids transport at the nanoscale, such as enhanced water transport in SWCNT or cation mobility in 2-nm silica nanochannels,[16,125] which may have a huge impact to address ever-increasing energy demands and environment issues. On the other hand, further development of such fabrication approaches will also expand nanofluidics applications in bio-related fields as nanochannels with feature size less than 5 nm are perfect tools for single molecule studies[306,315] as well as direct manipulation of physiological media.[125,309] The key

challenge here is how to define the sub-5 nm feature in a reliable and pre-designable way. The state-of-the-art of the laboratory fabrication, as summarized in Sec. VI B, has already demonstrated its ability in preparing ultra-fine nanostructures. Moreover, combined fabrication strategy, such as EBL plus ALD, could even provide possible solutions for nanofluidic device preparation with feature size down to sub-5 nm. Besides developing new approaches based on current mature techniques, one may also consider explore new fabrication method, especially based on recent advanced facilities. For example, the helium ion microscope (HIM), which uses a helium gas field ion source, is believed to be one of the most possible facilities for top-down nanofabrication directly achieving a feature size smaller than 1 nm.[316,317] HIM is capable of imaging, milling or gas-assisted material deposition with an ultra-fine resolution due to its high source brightness, low energy spread, and small diffraction effects. However, HIM is still in its early stages of development and needs further improvements to fabricate applicable nanofluidic devices for both fundamental studies and practical applications.

Nowadays, electrokinetics in some unconventional channels, like funnel or rhombus shaped, with feature size varied from nanometer to micrometer, are attracting broad attentions in nanofluidics because of many non-linear ion transport behaviors in these asymmetric structures.[6,17,142,220,225,228,315,318] However, the continuously varied feature size presents a serious fabrication challenge as either expensive mask/exposure system or lengthy process time is required for traditional lithography and direct-writing nanolithography, respectively. So far, the available solutions are the etching-and-deposition approach[318] and sacrificial layer releasing approach,[4] although their size controllability and integration reliability are far from the requirement and still need further improvements. Besides the challenge of achieving gradual-changing geometry, nanofluidics researchers also face difficulties in realizing heterogeneous nanofluidic devices with tunable surface properties. Several techniques including DLP,[5] sequentially patterning different oxides,[299] and packing different nanoparticles[249,250] have been invented to form nanofluidics diodes with opposite surface charge polarities. However, simpler and more scalable methods are still desired to further explore the fundamental of heterogeneous nanofluidics and expand its application as well. More importantly, further efforts are required to integrate nanofabrication process with traditional microfabrication techniques to realize the fluidic and electrical connections between the key nanoscale component and the supportive macroscopic world. Although many nanofabrication approaches reviewed in the paper are compatible with microfabrication (see discussion in Sec. VI C), some issues still exist in the present integration process, such as collapses in bonding, un-expected residues in sacrificial layer releasing or photoresist removal, and thus continuously call for efforts to improve the process reliability and yield.

Last but not the least, facile nanofabrication techniques with low cost, fast processes, and simple facility requirements, like soft-lithography in microfluidics, are still in high demand, especially for rapid prototyping of novel nanofluidics principles.[18,19,21,24] Cutting down the fabrication cost will be helpful to expand nanofluidic study to much broader research. However, present nanofabrication techniques that fulfilled the above requirements are usually suffering from poor size controllability and limited process integratability. A material that cherishes the same easy fabrication ability of PDMS but with a relatively larger Young's modulus, which means less collapse risk, might enable a soft-lithography typed nanofabrication approach for nanofluidic devices, such as the recent effort of using hard PDMS in nanofluidic device preparation.[25] Using nanomaterials, like nanotubes or nanoparticles, on the other hand, might provide a promising choice for nanofabrication approaches that satisfy the required criteria, if they can be formed to an organized nanocomponent in a predefined micro/macro structure by self-assembly or *in situ* synthesis. Recently, mesoporous silica film[319–321] that was prepared by directional synthesis might be a good candidate for facile nanofabrication based on nanomaterial strategy as it can be easy to manipulate and integrate with current PDMS-based microfluidic devices. The development of material science will keep providing more and more choices for facile nanofabrication. Researchers with interests in nanofluidics may pay close attention to related advancements.

Overall, with the advancement of nanofabrication techniques, it is foreseeable that more and more nanofluidic devices with high precise size controllability, unique geometrical

structures, controllable surface properties and more integrated powerful functions will be reported in the near future to further explore nanofluidics.

ACKNOWLEDGMENTS

[1]J. C. T. Eijkel and A. v. d. Berg, "Nanofluidics: What is it and what can we expect from it?" Microfluid. Nanofluid. **1**(3), 249–267 (2005).

[2]W. Sparreboom, A. van den Berg, and J. C. Eijkel, "Principles and applications of nanofluidic transport," Nat. Nanotechnol. **4**(11), 713–720 (2009).

[3]N. R. Tas, P. Mela, T. Kramer, J. W. Berenschot, and A. van den Berg, "Capillarity induced negative pressure of water plugs in nanochannels," Nano Lett. **3**(11), 1537–1540 (2003).

[4]C. Duan, R. Karnik, M. C. Lu, and A. Majumdar, "Evaporation-induced cavitation in nanofluidic channels," Proc. Natl. Acad. Sci. U.S.A. **109**(10), 3683–3693 (2012).

[5]R. Karnik, K. Castelino, C. H. Duan, and A. Majumdar, "Diffusion-limited patterning of molecules in nanofluidic channels," Nano Lett. **6**(8), 1735–1740 (2006).

[6]H. C. Chang and G. Yossifon, "Understanding electrokinetics at the nanoscale: A perspective," Biomicrofluidics **3**(1), 012001 (2009).

[7]D. Stein, M. Kruithof, and C. Dekker, "Surface-charge-governed ion transport in nanofluidic channels," Phys. Rev. Lett. **93**(3), 035901 (2004).

[8]J. O. Tegenfeldt, H. Cao, W. W. Reisner, C. Prinz, R. H. Austin, S. Y. Chou, E. C. Cox, and J. C. Sturm, "Stretching DNA in nanochannels," Biophys. J. **86**(1), 596A (2004).

[9]P. Abgrall and N. T. Nguyen, "Nanofluidic devices and their applications," Anal. Chem. **80**(7), 2326–2341 (2008).

[10]R. Schoch, J. Han, and P. Renaud, "Transport phenomena in nanofluidics," Rev. Mod. Phys. **80**(3), 839–883 (2008).

[11]D. Xia, J. Yan, and S. Hou, "Fabrication of nanofluidic biochips with nanochannels for applications in DNA analysis," Small **8**(18), 2787–2801 (2012).

[12]H. Daiguji, P. Yang, A. J. Szeri, and A. Majumdar, "Electrochemomechanical energy conversion in nanofluidic channels," Nano Lett. **4**(12), 2315–2321 (2004).

[13]D.-K. Kim, C. Duan, Y.-F. Chen, and A. Majumdar, "Power generation from concentration gradient by reverse electro-dialysis in ion-selective nanochannels," Microfluid. Nanofluid. **9**(6), 1215–1224 (2010).

[14]S. Moghaddam, E. Pengwang, Y. B. Jiang, A. R. Garcia, D. J. Burnett, C. J. Brinker, R. I. Masel, and M. A. Shannon, "An inorganic-organic proton exchange membrane for fuel cells with a controlled nanoscale pore structure," Nat. Nanotechnol. **5**(3), 230–236 (2010).

[15]S. J. Kim, S. H. Ko, K. H. Kang, and J. Han, "Direct seawater desalination by ion concentration polarization," Nat. Nanotechnol. **5**(4), 297–301 (2010).

[16]J. K. Holt, H. G. Park, Y. M. Wang, M. Stadermann, A. B. Artyukhin, C. P. Grigoropoulos, A. Noy, and O. Bakajin, "Fast mass transport through sub-2-nanometer carbon nanotubes," Science **312**(5776), 1034–1037 (2006).

[17]M. R. Powell, M. Sullivan, I. Vlassiouk, D. Constantin, O. Sudre, C. C. Martens, R. S. Eisenberg, and Z. S. Siwy, "Nanoprecipitation-assisted ion current oscillations," Nat. Nanotechnol. **3**(1), 51–57 (2008).

[18]B. D. Gates, Q. Xu, J. C. Love, D. B. Wolfe, and G. M. Whitesides, "Unconventional nanofabrication," Annu. Rev. Mater. Res. **34**(1), 339–372 (2004).

[19]B. D. Gates, Q. Xu, M. Stewart, D. Ryan, C. G. Willson, and G. M. Whitesides, "New approaches to nanofabrication: Molding, printing, and other techniques," Chem. Rev. **105**(4), 1171–1196 (2005).

[20]J. L. Perry and S. G. Kandlikar, "Review of fabrication of nanochannels for single phase liquid flow," Microfluid. Nanofluid. **2**(3), 185–193 (2005).

[21]D. Mijatovic, J. C. Eijkel, and A. van den Berg, "Technologies for nanofluidic systems: Top-down vs. bottom-up–a review," Lab Chip **5**(5), 492–500 (2005).

[22]C. Dekker, "Solid-state nanopores," Nat. Nanotechnol. **2**(4), 209–215 (2007).

[23]S. Prakash, A. Piruska, E. N. Gatimu, P. W. Bohn, J. V. Sweedler, and M. A. Shannon, "Nanofluidic: Systems and applications," IEEE Sens. J. **8**(5), 441–450 (2008).

[24]Y. Chen and A. Pepin, "Nanofabrication: Concentional and nonconventional methods," Electrophoresis **22**, 187–207 (2001).

[25]J. M. Perry, K. Zhou, Z. D. Harms, and S. C. Jacobson, "Ion transport in nanofluidic funnels," ACS Nano **4**(7), 3897–3902 (2010).

[26]S. H. Kim, Y. Cui, M. J. Lee, S. W. Nam, D. Oh, S. H. Kang, Y. S. Kim, and S. Park, "Simple fabrication of hydrophilic nanochannels using the chemical bonding between activated ultrathin PDMS layer and cover glass by oxygen plasma," Lab Chip **11**(2), 348–353 (2011).

[27]R. Yokokawa, Y. Yoshida, S. Takeuchi, T. Kon, and H. Fujita, "Unidirectional transport of a bead on a single microtubule immobilized in a submicrometre channel," Nanotechnology **17**(1), 289–294 (2006).

[28]A. Hibara, T. Saito, H. B. Kim, M. Tokeshi, T. Ooi, M. Nakao, and T. Kitamori, "Nanochannels on a fused-silica microchip and liquid properties investigation by time-resolved fluorescence measurements," Anal. Chem. **74**(24), 6170–6176 (2002).

[29]T. Tsukahara, W. Mizutani, K. Mawatari, and T. Kitamori, "NMR studies of structure and dynamics of liquid molecules confined in extended nanospaces," J. Phys. Chem. B **113**(31), 10808–10816 (2009).

[30]E. Tamaki, A. Hibara, H. B. Kim, M. Tokeshi, and T. Kitamori, "Pressure-driven flow control system for nanofluidic chemical process," J. Chromatogr. A **1137**(2), 256–262 (2006).

[31]Z. D. Harms, K. B. Mogensen, P. S. Nunes, K. Zhou, B. W. Hildenbrand, I. Mitra, Z. Tan, A. Zlotnick, J. P. Kutter, and S. C. Jacobson, "Nanofluidic devices with two pores in series for resistive-pulse sensing of single virus capsids," Anal. Chem. **83**(24), 9573–9578 (2011).

[32]S. L. Levy, J. T. Mannion, J. Cheng, C. H. Reccius, and H. G. Craighead, "Entropic unfolding of DNA molecules in nanofluidic channels," Nano Lett. **8**(11), 3839–3844 (2008).

[33]R. Riehn, R. H. Austin, and J. C. Sturm, "A nanofluidic railroad switch for DNA," Nano Lett. **6**(9), 1973–1976 (2006).

[34]W. Reisner, J. Beech, N. Larsen, H. Flyvbjerg, A. Kristensen, and J. Tegenfeldt, "Nanoconfinement-enhanced conformational response of single DNA molecules to changes in ionic environment," Phys. Rev. Lett. **99**(5), 058302 (2007).

[35]S. W. Nam, M. H. Lee, S. H. Lee, D. J. Lee, S. M. Rossnagel, and K. B. Kim, "Sub-10-nm nanochannels by self-sealing and self-limiting atomic layer deposition," Nano Lett. **10**(9), 3324–3329 (2010).

[36]M. Fouad, M. Yavuz, and B. Cui, "Nanofluidic channels fabricated by e-beam lithography and polymer reflow sealing," J. Vac. Sci. Technol. B **28**(6), C6I11–C6I13 (2010).

[37]C. K. Tung, R. Riehn, and R. H. Austin, "Complementary metal oxide semiconductor compatible fabrication and characterization of parylene-C covered nanofluidic channels with integrated nanoelectrodes," Biomicrofluidics **3**(3), 031101 (2009).

[38]A. A. Tseng, "Recent developments in nanofabrication using focused ion beams," Small **1**(10), 924–939 (2005).

[39]A. A. Tseng, "Recent developments in micromilling using focused ion beam technology," J. Micromech. Microeng. **14**(4), R15–R34 (2004).

[40]P. Chen, J. J. Gu, E. Brandin, Y. R. Kim, Q. Wang, and D. Branton, "Probing single DNA molecule transport using fabricated nanopores," Nano Lett. **4**(11), 2293–2298 (2004).

[41]C. Danelon, C. Santschi, J. Brugger, and H. Vogel, "Fabrication and functionalization of nanochannels by electron-beam-induced silicon oxide deposition," Langmuir **22**(25), 10711–10715 (2006).

[42]V. Mussi, P. Fanzio, L. Repetto, G. Firpo, P. Scaruffi, S. Stigliani, G. P. Tonini, and U. Valbusa, "DNA-functionalized solid state nanopore for biosensing," Nanotechnology **21**(14), 145102 (2010).

[43]H. D. Tong, H. V. Jansen, V. J. Gadgil, C. G. Bostan, E. Berenschot, C. J. M. van Rijn, and M. Elwenspoek, "Silicon nitride nanosieve membrane," Nano Lett. **4**(2), 283–287 (2004).

[44]Z. P. Tian, K. Lu, and B. Chen, "Unique nanopore pattern formation by focused ion beam guided anodization," Nanotechnology **21**(40), 405301 (2010).

[45]D. M. Cannon, B. R. Flachsbart, M. A. Shannon, J. V. Sweedler, and P. W. Bohn, "Fabrication of single nanofluidic channels in poly(methylmethacrylate) films via focused-ion beam milling for use as molecular gates," Appl. Phys. Lett. **85**(7), 1241–1243 (2004).

[46]A. A. Tseng, I. A. Insua, J. S. Park, B. Li, G. P. Vakanas, "Milling of submicron channels on gold layer using double charged arsenic ion beam," J. Vac. Sci. Technol. B **22**(1), 82–89 (2004).

[47]L. Guan, K. Peng, Y. Yang, X. Qiu, and C. Wang, "The nanofabrication of polydimethylsiloxane using a focused ion beam," Nanotechnology **20**(14), 145301 (2009).

[48]L. Frey, C. Lehrer, and H. Ryssel, "Nanoscale effects in focused ion beam processing," Appl. Phys. A: Mater. Sci. Process. **76**(7), 1017–1023 (2003).

[49]H.-W. Li, D.-J. Kang, M. G. Blamire, and W. T. Huck, "Focused ion beam fabrication of silicon print masters," Nanotechnology **14**, 220–223 (2003).

[50]T. Yamamoto and T. Fujii, "Nanofluidic single-molecule sorting of DNA: A new concept in separation and analysis of biomolecules towards ultimate level performance," Nanotechnology **21**(39), 395502 (2010).

[51]L. D. Menard and J. M. Ramsey, "Fabrication of sub-5 nm nanochannels in insulating substrates using focused ion beam milling," Nano Lett. **11**(2), 512–517 (2011).

[52]T. Maleki, S. Mohammadi, and B. Ziaie, "A nanofluidic channel with embedded transverse nanoelectrodes," Nanotechnology **20**(10), 105302 (2009).

[53]A. A. Tseng, I. A. Insua, J.-S. Park, and C. D. Chen, "Milling yield estimation in focused ion beam milling of two-layer substrates," J. Micromech. Microeng. **15**(1), 20–28 (2005).

[54]E. Angeli, C. Manneschi, L. Repetto, G. Firpo, and U. Valbusa, "DNA manipulation with elastomeric nanostructures fabricated by soft-moulding of a FIB-patterned stamp," Lab Chip **11**(15), 2625–2629 (2011).

[55]P. Fanzio, V. Mussi, C. Manneschi, E. Angeli, G. Firpo, L. Repetto, and U. Valbusa, "DNA detection with a polymeric nanochannel device," Lab Chip **11**(17), 2961–2966 (2011).

[56]J. Wu, R. Chantiwas, A. Amirsadeghi, S. A. Soper, and S. Park, "Complete plastic nanofluidic devices for DNA analysis via direct imprinting with polymer stamps," Lab Chip **11**(17), 2984–2989 (2011).

[57]L. J. Guo, "Nanoimprint lithography: Methods and material requirements," Adv. Mater. **19**(4), 495–513 (2007).

[58]X. Li, X. Wang, J. Jin, Q. Tang, Y. Tian, S. Fu, and Z. Cui, "Fabrication of micro/nano fluidic system combining hybrid mask-mould lithography with thermal bonding," Microelectron. Eng. **87**(5–8), 722–725 (2010).

[59]B. Yang, V. R. Dukkipati, D. Li, B. L. Cardozo, S. W. Pang, "Stretching and selective immobilization of DNA in SU-8 micro- and nanochannels," J. Vac. Sci. Technol. B **25**(6), 2352–2356 (2007).

[60]L. H. Thamdrup, A. Klukowska, and A. Kristensen, "Stretching DNA in polymer nanochannels fabricated by thermal imprint in PMMA," Nanotechnology **19**(12), 125301 (2008).

[61]Y. H. Cho, J. Park, H. Park, X. Cheng, B. J. Kim, and A. Han, "Fabrication of high-aspect-ratio polymer nanochannels using a novel Si nanoimprint mold and solvent-assisted sealing," Microfluid. Nanofluid. **9**(2–3), 163–170 (2009).

[62]Q. Xia, K. J. Morton, R. H. Austin, and S. Y. Chou, "Sub-10 nm self-enclosed self-limited nanofluidic channel arrays," Nano Lett. **8**(11), 3830–3833 (2008).

[63]L. J. Guo, X. Cheng, and C. F. Chou, "Fabrication of size-controllable nanofluidic channels by nanoimprinting and its application for DNA stretching," Nano Lett. **4**(1), 69–73 (2004).

[64]R. Chantiwas, M. L. Hupert, S. R. Pullagurla, S. Balamurugan, J. Tamarit-Lopez, S. Park, P. Datta, J. Goettert, Y. K. Cho, and S. A. Soper, "Simple replication methods for producing nanoslits in thermoplastics and the transport dynamics of double-stranded DNA through these slits," Lab Chip **10**(23), 3255–3264 (2010).

[65]M. B. Mikkelsen, A. A. Letailleur, E. Sondergard, E. Barthel, J. Teisseire, R. Marie, and A. Kristensen, "All-silica nanofluidic devices for DNA-analysis fabricated by imprint of sol-gel silica with silicon stamp," Lab Chip **12**(2), 262–267 (2012).

[66]N. R. Hendricks, J. J. Watkins, and K. R. Carter, "Formation of hierarchical silica nanochannels through nanoimprint lithography." J. Mater. Chem. **21**(37), 14213–14218 (2011).

[67]R. M. Reano and S. W. Pang, "Sealed three-dimensional nanochannels," J. Vac. Sci. Technol. B **23**(6), 2995–2999 (2005).

[68]X. Liang and S. Y. Chou, "Nanogap detector inside nanofluidic channel for fast real-time label-free DNA analysis," Nano Lett. **8**(5), 1472–1476 (2008).

[69]D. Xia, Z. Ku, S. C. Lee, and S. R. Brueck, "Nanostructures and functional materials fabricated by interferometric lithography," Adv. Mater. **23**(2), 147–179 (2011).

[70]Y. J. Oh, T. C. Gamble, D. Leonhardt, C. H. Chung, S. R. Brueck, C. F. Ivory, G. P. Lopez, D. N. Petsev, and S. M. Han, "Monitoring FET flow control and wall adsorption of charged fluorescent dye molecules in nanochannels integrated into a multiple internal reflection infrared waveguide," Lab Chip **8**(2), 251–258 (2008).

[71]Y. J. Oh, D. Bottenus, C. F. Ivory, and S. M. Han, "Impact of leakage current and electrolysis on FET flow control and pH changes in nanofluidic channels," Lab Chip **9**(11), 1609–1617 (2009).

[72]M. J. O'Brien, P. Bisong, L. K. Ista, E. M. Rabinovich, A. L. Garcia, S. S. Sibbett, G. P. Lopez, and S. R. J. Brueck, "Fabrication of an integrated nanofluidic chip using interferometric lithography," J. Vac. Sci. Technol. B **21**(6), 2941–2945 (2003).

[73]D. Bottenus, Y. J. Oh, S. M. Han, and C. F. Ivory, "Experimentally and theoretically observed native pH shifts in a nanochannel array," Lab Chip **9**(2), 219–231 (2009).

[74]A. L. Garcia, L. K. Ista, D. N. Petsev, M. J. O'Brien, P. Bisong, A. A. Mammoli, S. R. Brueck, and G. P. Lopez, "Electrokinetic molecular separation in nanoscale fluidic channels," Lab Chip **5**(11), 1271–1276 (2005).

[75]Y. J. Oh, A. L. Garcia, D. N. Petsev, G. P. Lopez, S. R. Brueck, C. F. Ivory, and S. M. Han, "Effect of wall-molecule interactions on electrokinetic transport of charged molecules in nanofluidic channels during FET flow control," Lab Chip **9**(11), 1601–1608 (2009).

[76]Y. Zhang, T. C. Gamble, A. Neumann, G. P. Lopez, S. R. Brueck, and D. N. Petsev, "Electric field control and analyte transport in Si/SiO$_2$ fluidic nanochannels," Lab Chip **8**(10), 1671–1675 (2008).

[77]Y. Kim, K. S. Kim, K. L. Kounovsky, R. Chang, G. Y. Jung, J. J. dePablo, K. Jo, and D. C. Schwartz, "Nanochannel confinement: DNA stretch approaching full contour length," Lab Chip **11**(10), 1721–1729 (2011).

[78]N. M. Elman, K. Daniel, F. Jalali-Yazdi, and M. J. Cima, "Super permeable nano-channel membranes defined with laser interferometric lithography," Microfluid. Nanofluid. **8**(4), 557–563 (2009).

[79]H. M. Chen, L. Pang, M. S. Gordon, and Y. Fainman, "Real-time template-assisted manipulation of nanoparticles in a multilayer nanofluidic chip," Small **7**(19), 2750–2757 (2011).

[80]G. Zhang and D. Wang, "Colloidal lithography–The art of nanochemical patterning," Chem. Asian J. **4**(2), 236–245 (2009).

[81]Y. Li, W. Cai, and G. Duan, "Ordered micro/nanostructured arrays based on the monolayer colloidal crystals," Chem. Mater. **20**(3), 615–624 (2008).

[82]N. Vogel, C. K. Weiss, and K. Landfester, "From soft to hard: The generation of functional and complex colloidal monolayers for nanolithography," Soft Matter **8**(15), 4044 (2012).

[83]A. V. Whitney, B. D. Myers, and R. P. Van Duyne, "Sub-100 nm triangular nanopores fabricated with the reactive ion etching variant of nanosphere lithography and angle-resolved nanosphere lithography," Nano Lett. **4**(8), 1507–1511 (2004).

[84]N. Denkov, O. Velev, P. Kralchevski, I. Ivanov, H. Yoshimura, and K. Nagayama, "Mechanism of formation of two-dimensional crystals from latex particles on substrates," Langmuir **8**(12), 3183–3190 (1992).

[85]J. Huang, F. Kim, A. R. Tao, S. Connor, and P. Yang, "Spontaneous formation of nanoparticle stripe patterns through dewetting," Nature Mater. **4**(12), 896–900 (2005).

[86]C.-M. Hsu, S. T. Connor, M. X. Tang, and Y. Cui, "Wafer-scale silicon nanopillars and nanocones by Langmuir–Blodgett assembly and etching," Appl. Phys. Lett. **93**(13), 133109 (2008).

[87]S. Jeong, L. Hu, H. R. Lee, E. Garnett, J. W. Choi, and Y. Cui, "Fast and scalable printing of large area monolayer nanoparticles for nanotexturing applications," Nano Lett. **10**(8), 2989–2994 (2010).

[88]Z. X. Lu, A. Namboodiri, and M. M. Collinson, "Self-supporting nanopore membranes with controlled pore size and shape," ACS Nano **2**(5), 993–999 (2008).

[89]M. B. Stern, M. W. Geis, and J. E. Curtin, "Nanochannel fabrication for chemical sensors," J. Vac. Sci. Technol. B **15**(6), 2887–2891 (1997).

[90]R. Karnik, R. Fan, M. Yue, D. Li, P. Yang, and A. Majumdar, "Electrostatic control of ions and molecules in nanofluidic transistors," Nano Lett. **5**(5), 943–948 (2005).

[91]R. Karnik, K. Castelino, R. Fan, P. Yang, and A. Majumdar, "Effects of biological reactions and modifications on conductance of nanofluidic channels," Nano Lett. **5**(9), 1638–1642 (2005).

[92]R. Karnik, K. Castelino, and A. Majumdar, "Field-effect control of protein transport in a nanofluidic transistor circuit," Appl. Phys. Lett. **88**(12), 123114 (2006).

[93]R. Karnik, C. Duan, K. Castelino, H. Daiguji, and A. Majumdar, "Rectification of ionic current in a nanofluidic diode," Nano Lett. **7**(3), 547–551 (2007).

[94]L. J. Cheng and L. J. Guo, "Rectified ion transport through concentration gradient in homogeneous silica nanochannels," Nano Lett. **7**(10), 3165–3171 (2007).

[95]R. A. Barton, B. Ilic, S. S. Verbridge, B. R. Cipriany, J. M. Parpia, and H. G. Craighead, "Fabrication of a nanomechanical mass sensor containing a nanofluidic channel," Nano Lett. **10**(6), 2058–2063 (2010).

[96]T. S. Hug, N. F. de Rooij, and U. Staufer, "Fabrication and electroosmotic flow measurements in micro- and nanofluidic channels," Microfluid. Nanofluid. **2**(2), 117–124 (2006).

[97]C. Shen, V. R. S. S. Mokkapati, H. T. M. Pham, and P. M. Sarro, "Micromachined nanofiltration modules for lab-on-a-chip applications," J. Micromech. Microeng. **22**(2), 025003 (2012).

[98] J. C. Eijkel, J. Bomer, N. R. Tas, and A. van den Berg, "1-D nanochannels fabricated in polyimide," Lab Chip **4**(3), 161–163 (2004).

[99] M. N. Hamblin, A. R. Hawkins, D. Murray, D. Maynes, M. L. Lee, A. T. Woolley, and H. D. Tolley, "Capillary flow in sacrificially etched nanochannels," Biomicrofluidics **5**(2), 021103 (2011).

[100] K. P. Nichols, J. C. Eijkel, and H. J. Gardeniers, "Nanochannels in SU-8 with floor and ceiling metal electrodes and integrated microchannels," Lab Chip **8**(1), 173–175 (2008).

[101] M. A. Zevenbergen, P. S. Singh, E. D. Goluch, B. L. Wolfrum, and S. G. Lemay, "Stochastic sensing of single molecules in a nanofluidic electrochemical device," Nano Lett. **11**(7), 2881–2886 (2011).

[102] M. N. Hamblin, J. Xuan, D. Maynes, H. D. Tolley, D. M. Belnap, A. T. Woolley, M. L. Lee, and A. R. Hawkins, "Selective trapping and concentration of nanoparticles and viruses in dual-height nanofluidic channels," Lab Chip **10**(2), 173–178 (2010).

[103] W. Sparreboom, J. C. Eijkel, J. Bomer, and A. van den Berg, "Rapid sacrificial layer etching for the fabrication of nanochannels with integrated metal electrodes," Lab Chip **8**(3), 402–407 (2008).

[104] R. Sordan, A. Miranda, F. Traversi, D. Colombo, D. Chrastina, G. Isella, M. Masserini, L. Miglio, K. Kern, and K. Balasubramanian, "Vertical arrays of nanofluidic channels fabricated without nanolithography," Lab Chip **9**(11), 1556–1560 (2009).

[105] H. Zeng, Z. Wan, and A. D. Feinerman, "Fabrication of micro/nano fluidic channels with sacrificial galvanic coupled metals," Nanotechnology **17**(13), 3183–3188 (2006).

[106] C. Peng and S. W. Pang, "Three-dimensional nanochannels formed by fast etching of polymer," J. Vac. Sci. Technol. B **24**(4), 1941–1946 (2006).

[107] S. Wang, X. Hu, and L. J. Lee, "Electrokinetics induced asymmetric transport in polymeric nanonozzles," Lab Chip **8**(4), 573–581 (2008).

[108] L. M. Bellan, E. A. Strychalski, and H. G. Craighead, "Nanochannels fabricated in polydimethylsiloxane using sacrificial electrospun polyethylene oxide nanofibers," J. Vac. Sci. Technol. B **26**(5), 1728–1731 (2008).

[109] S. Lee, K. Limkrailassiri, Y. Gao, C. Chang, and L. W. Lin, "Chip-to-chip fluidic connectors via near-field electrospinning," in *Proceedings of IEEE MicroElectroMechanical Systems* (IEEE, 2007), pp. 252–255.

[110] J. Guan, P. E. Boukany, O. Hemminger, N. R. Chiou, W. Zha, M. Cavanaugh, and L. J. Lee, "Large laterally ordered nanochannel arrays from DNA combing and imprinting," Adv. Mater. **22**(36), 3997–4001 (2010).

[111] P. E. Boukany, A. Morss, W. C. Liao, B. Henslee, H. Jung, X. Zhang, B. Yu, X. Wang, Y. Wu, L. Li, K. Gao, X. Hu, X. Zhao, O. Hemminger, W. Lu, G. P. Lafyatis, and L. J. Lee, "Nanochannel electroporation delivers precise amounts of biomolecules into living cells," Nat. Nanotechnol. **6**(11), 747–754 (2011).

[112] N. R. Devlin and D. K. Brown, "Fabricating millimeter to nanometer sized cavities concurrently for nanofluidic devices," J. Vac. Sci. Technol. B **28**(6), C6I7–C6I10 (2010).

[113] N. R. Devlin, D. K. Brown, and P. A. Kohl, "Patterning decomposable polynorbornene with electron beam lithography to create nanochannels," J. Vac. Sci. Technol. B **27**(6), 2508–2511 (2009).

[114] C. K. Harnett, G. W. Coates, and H. G. Craighead, "Heat-depolymerizable polycarbonates as electron beam patternable sacrificial layers for nanofluidics," J. Vac. Sci. Technol. B **19**(6), 2842–2845 (2001).

[115] X. T. Huang, C. Gupta, and S. Pennathur, "A novel fabrication method for centimeter-long surface-micromachined nanochannels," J. Micromech. Microeng. **20**(1), 015040 (2010).

[116] H. T. Hoang, H. D. Tong, I. M. Segers-Nolten, N. R. Tas, V. Subramaniam, and M. C. Elwenspoek, "Wafer-scale thin encapsulated two-dimensional nanochannels and its application toward visualization of single molecules," J. Colloid Interface Sci. **367**(1), 455–459 (2012).

[117] A. Grattoni, D. Fine, E. Zabre, A. Ziemys, J. Gill, Y. Mackeyev, M. A. Cheney, D. C. Danila, S. Hosali, L. J. Wilson, F. Hussain, and M. Ferrari, "Gated and near-surface diffusion of charged fullerenes in nanochannels," ACS Nano **5**(12), 9382–9391 (2011).

[118] H. T. Hoang, I. M. Segers-Nolten, J. W. Berenschot, M. J. de Boer, N. R. Tas, J. Haneveld, and M. C. Elwenspoek, "Fabrication and interfacing of nanochannel devices for single-molecule studies," J. Micromech. Microeng. **19**(6), 065017 (2009).

[119] J. Haneveld, H. Jansen, E. Berenschot, N. Tas, and M. Elwenspoek, "Wet anisotropic etching for fluidic 1D nanochannels," J. Micromech. Microeng. **13**(4), S62–S66 (2003).

[120] M. Wang, N. Jing, I. H. Chou, G. L. Cote, and J. Kameoka, "An optofluidic device for surface enhanced Raman spectroscopy," Lab Chip **7**(5), 630–632 (2007).

[121] Y. C. Wang and J. Han, "Pre-binding dynamic range and sensitivity enhancement for immuno-sensors using nanofluidic preconcentrator," Lab Chip **8**(3), 392–394 (2008).

[122] R. B. Veenhuis, E. J. van der Wouden, J. W. van Nieuwkasteele, A. van den Berg, and J. C. Eijkel, "Field-effect based attomole titrations in nanoconfinement," Lab Chip **9**(24), 3472–3480 (2009).

[123] D. Kim, A. Raj, L. Zhu, R. I. Masel, and M. A. Shannon, "Non-equilibrium electrokinetic micro/nano fluidic mixer," Lab Chip **8**(4), 625–628 (2008).

[124] S. J. Lee and D. Kim, "Millisecond-order rapid micromixing with non-equilibrium electrokinetic phenomena," Microfluid. Nanofluid. **12**, 897–906 (2011).

[125] C. Duan and A. Majumdar, "Anomalous ion transport in 2-nm hydrophilic nanochannels," Nat. Nanotechnol. **5**(12), 848–852 (2010).

[126] P. Abgrall, L. N. Low, and N. T. Nguyen, "Fabrication of planar nanofluidic channels in a thermoplastic by hot-embossing and thermal bonding," Lab Chip **7**(4), 520–522 (2007).

[127] K.-D. Huang and R.-J. Yang, "Formation of ionic depletion/enrichment zones in a hybrid micro-/nano-channel," Microfluid. Nanofluid. **5**(5), 631–638 (2008).

[128] Z. Xu, J.-K. Wen, C. Liu, J.-S. Liu, L.-Q. Du, and L.-D. Wang, "Research on forming and application of U-form glass micro-nanofluidic chip with long nanochannels," Microfluid. Nanofluid. **7**(3), 423–429 (2009).

[129] L. Shui, A. Berg, and J. C. T. Eijkel, "Scalable attoliter monodisperse droplet formation using multiphase nano-microfluidics," Microfluid. Nanofluid. **11**(1), 87–92 (2011).

[130] Q. S. Pu, J. S. Yun, H. Temkin, and S. R. Liu, "Ion-enrichment and ion-depletion effect of nanochannel structures," Nano Lett. **4**(6), 1099–1103 (2004).

[131] S. Liu, Q. Pu, L. Gao, C. Korzeniewski, and C. Matzke, "From nanochannel-induced proton conduction enhancement to a nanochannel-based fuel cell," Nano Lett. **5**(7), 1389–1393 (2005).

[132] R. B. Schoch, L. F. Cheow, and J. Han, "Electrical detection of fast reaction kinetics in nanochannels with an induced flow," Nano Lett. **7**(12), 3895–3900 (2007).

[133] J. J. Jones, J. R. van der Maarel, and P. S. Doyle, "Effect of nanochannel geometry on DNA structure in the presence of macromolecular crowding agent," Nano Lett. **11**(11), 5047–5053 (2011).

[134] I. H. Chou, M. Benford, H. T. Beier, G. L. Cote, M. Wang, N. Jing, J. Kameoka, and T. A. Good, "Nanofluidic biosensing for beta-amyloid detection using surface enhanced Raman spectroscopy," Nano Lett. **8**(6), 1729–1735 (2008).

[135] D. Stein, Z. Deurvorst, F. H. van der Heyden, W. J. Koopmans, A. Gabel, and C. Dekker, "Electrokinetic concentration of DNA polymers in nanofluidic channels," Nano Lett. **10**(3), 765–772 (2010).

[136] P. Mao and J. Han, "Fabrication and characterization of 20 nm planar nanofluidic channels by glass-glass and glass-silicon bonding," Lab Chip **5**(8), 837–844 (2005).

[137] K. Pappaert, J. Biesemans, D. Clicq, S. Vankrunkelsven, and G. Desmet, "Measurements of diffusion coefficients in 1-D micro- and nanochannels using shear-driven flows," Lab Chip **5**(10), 1104–1110 (2005).

[138] N. F. Y. Durand, A. Bertsch, M. Todorova, and P. Renaud, "Direct measurement of effective diffusion coefficients in nanochannels using steady-state dispersion effects," Appl. Phys. Lett. **91**(20), 203106 (2007).

[139] N. F. Durand and P. Renaud, "Label-free determination of protein-surface interaction kinetics by ionic conductance inside a nanochannel," Lab Chip **9**(2), 319–324 (2009).

[140] A. Plecis, R. B. Schoch, and P. Renaud, "Ionic transport phenomena in nanofluidics: Experimental and theoretical study of the exclusion-enrichment effect on a chip," Nano Lett. **5**(6), 1147–1155 (2005).

[141] R. B. Schoch, A. Bertsch, and P. Renaud, "pH-controlled diffusion of proteins with different pI values across a nanochannel on a chip," Nano Lett. **6**(3), 543–547 (2006).

[142] G. Yossifon, Y.-C. Chang, and H.-C. Chang, "Rectification, gating voltage, and interchannel communication of nanoslot arrays due to asymmetric entrance space charge polarization," Phys. Rev. Lett. **103**(15), 154502 (2009).

[143] V. R. Mokkapati, V. Di Virgilio, C. Shen, J. Mollinger, J. Bastemeijer, and A. Bossche, "DNA tracking within a nanochannel: Device fabrication and experiments," Lab Chip **11**(16), 2711–2719 (2011).

[144] H. T. Hoang, I. M. Segers-Nolten, N. R. Tas, J. W. van Honschoten, V. Subramaniam, and M. C. Elwenspoek, "Analysis of single quantum-dot mobility inside 1D nanochannel devices," Nanotechnology **22**(27), 275201 (2011).

[145] K. M. van Delft, J. C. Eijkel, D. Mijatovic, T. S. Druzhinina, H. Rathgen, N. R. Tas, A. van den Berg, and F. Mugele, "Micromachined Fabry-Perot interferometer with embedded nanochannels for nanoscale fluid dynamics," Nano Lett. **7**(2), 345–350 (2007).

[146] M. Krishnan, I. Monch, and P. Schwille, "Spontaneous stretching of DNA in a two-dimensional nanoslit," Nano Lett. **7**(5), 1270–1275 (2007).

[147] F. Persson, L. H. Thamdrup, M. B. L. Mikkelsen, S. E. Jaarlgard, P. Skafte-Pedersen, H. Bruus, A. Kristensen, "Double thermal oxidation scheme for the fabrication of SiO$_2$ nanochannels," Nanotechnology **18**(24), 245301 (2007).

[148] A. Grattoni, E. De Rosa, S. Ferrati, Z. Wang, A. Gianesini, X. Liu, F. Hussain, R. Goodall, and M. Ferrari, "Analysis of a nanochanneled membrane structure through convective gas flow," J. Micromech. Microeng. **19**(11), 115018 (2009).

[149] C. Wu, Z. Jin, H. Wang, H. Ma, and Y. Wang, "Design and fabrication of a nanofluidic channel by selective thermal oxidation and etching back of silicon dioxide made on a silicon substrate," J. Micromech. Microeng. **17**(12), 2393–2397 (2007).

[150] D. Fine, A. Grattoni, S. Hosali, A. Ziemys, E. De Rosa, J. Gill, R. Medema, L. Hudson, M. Kojic, M. Milosevic, L. Brousseau Iii, R. Goodall, M. Ferrari, and X. Liu, "A robust nanofluidic membrane with tunable zero-order release for implantable dose specific drug delivery," Lab Chip **10**(22), 3074–3083 (2010).

[151] D. Fine, A. Grattoni, E. Zabre, F. Hussein, M. Ferrari, and X. Liu, "A low-voltage electrokinetic nanochannel drug delivery system," Lab Chip **11**(15), 2526–2534 (2011).

[152] P. M. Sinha, G. Valco, S. Sharma, X. Liu, and M. Ferrari, "Nanoengineered device for drug delivery application," Nanotechnology **15**(10), S585–S589 (2004).

[153] C. R. Song and P. S. Wang, "Fabrication of sub-10 nm planar nanofluidic channels through native oxide etch and anodic wafer bonding," IEEE Trans. Nanotechnol. **9**(2), 138–141 (2010).

[154] W. P. Shih, C. Y. Hui, and N. C. Tien, "Collapse of microchannels during anodic bonding: Theory and experiments," J. Appl. Phys. **95**(5), 2800–2808 (2004).

[155] J. Haneveld, N. R. Tas, N. Brunets, H. V. Jansen, and M. Elwenspoek, "Capillary filling of sub-10 nm nanochannels," J. Appl. Phys. **104**(1), 014309 (2008).

[156] H. Y. Wang, R. S. Foote, S. C. Jacobson, J. H. Schneibel, and J. M. Ramsey, "Low temperature bonding for microfabrication of chemical analysis devices," Sens. Actuators B **45**(3), 199–207 (1997).

[157] T. P. Burg, M. Godin, S. M. Knudsen, W. Shen, G. Carlson, J. S. Foster, K. Babcock, and S. R. Manalis, "Weighing of biomolecules, single cells and single nanoparticles in fluid," Nature **446**(7139), 1066–1069 (2007).

[158] J. Lee, W. Shen, K. Payer, T. P. Burg, and S. R. Manalis, "Toward attogram mass measurements in solution with suspended nanochannel resonators," Nano Lett. **10**(7), 2537–2542 (2010).

[159] F. Devreux, P. Barboux, M. Filoche, and B. Sapoval, "A simplified model for glass dissolution in water," J. Mater. Sci. **36**(6), 1331–1341 (2001).

[160] B. Ilic, D. Czaplewski, M. Zalalutdinov, B. Schmidt, and H. G. Craighead, "Fabrication of flexible polymer tubes for micro and nanofluidic applications," J. Vac. Sci. Technol. B **20**(6), 2459–2465 (2002).

[161] C. C. Wong, A. Agarwal, N. Balasubramanian, and D. L. Kwong, "Fabrication of self-sealed circular nano/microfluidic channels in glass substrates," Nanotechnology **18**(13), 135304 (2007).

[162] L. Ji, J. K. Kim, Q. Ji, K. N. Leung, Y. Chen, and R. A. Gough, "Conformal metal thin-film coatings in high-aspect-ratio trenches using a self-sputtered rf-driven plasma source," J. Vac. Sci. Technol. B **25**(4), 1227–1230 (2007).

[163] P. Mao and J. Han, "Massively-parallel ultra-high-aspect-ratio nanochannels as mesoporous membranes," Lab Chip **9**(4), 586–591 (2009).

[164] J. C. Love, K. E. Paul, and G. M. Whitesides, "Fabrication of nanometer-scale features by controlled isotropic wet chemical etching," Adv. Mater. **13**(8), 604–607 (2001).

[165]L. Q. Chen, M. B. Chan-Park, Y. H. Yan, Q. Zhang, C. M. Li, and J. Zhang, "High aspect ratio silicon nanomoulds for UV embossing fabricated by directional thermal oxidation using an oxidation mask," Nanotechnology **18**(35), 355307 (2007).

[166]L. Q. Chen, M. B. Chan-Park, C. Yang, and Q. Zhang, "The residual pattern of double thin-film over-etching for the fabrication of continuous patterns with dimensions varying from 50 nm to millimeters over a large area," Nanotechnology **19**(15), 155301 (2008).

[167]Q. Xie, Q. Zhou, F. Xie, J. Sang, W. Wang, H. A. Zhang, W. Wu, and Z. Li, "Wafer-scale fabrication of high-aspect ratio nanochannels based on edge-lithography technique," Biomicrofluidics **6**(1), 016502 (2012).

[168]H. Y. Mao, W. G. Wu, Y. L. Zhang, G. Zhai, and J. Xu, "Fabrication of high-compact nanowires using alternating photoresist ashing and spacer technology," J. Micromech. Microeng. **20**(8), 085029 (2010).

[169]R. A. Smith, K. Goldman, W. H. Fissell, A. J. Fleischman, C. A. Zorman, and S. Roy, "Removal of endotoxin from deionized water using micromachined silicon nanopore membranes," J. Micromech. Microeng. **21**(5), 054029 (2011).

[170]C. Lee, E. H. Yang, N. V. Myung, and T. George, "A nanochannel fabrication technique without nanolithography," Nano Lett. **3**(10), 1339–1340 (2003).

[171]N. R. Tas, J. W. Berenschot, P. Mela, H. V. Jansen, M. Elwenspoek, and A. van den Berg, "2D-confined nanochannels fabricated by conventional micromachining," Nano Lett. **2**(9), 1031–1032 (2002).

[172]K. Tybrandt, R. Forchheimer, and M. Berggren, "Logic gates based on ion transistors," Nat. Commun. **3**, 871 (2012).

[173]E. O. Gabrielsson, K. Tybrandt, and M. Berggren, "Ion diode logics for pH control," Lab Chip **12**(14), 2507–2513 (2012).

[174]H. Kim, J. Kim, E. G. Kim, A. J. Heinz, S. Kwon, and H. Chun, "Optofluidic *in situ* maskless lithography of charge selective nanoporous hydrogel for DNA preconcentration," Biomicrofluidics **4**(4), 043014 (2010).

[175]P. Kim, S. J. Kim, J. Han, and K. Y. Suh, "Stabilization of ion concentration polarization using a heterogeneous nanoporous junction," Nano Lett. **10**(1), 16–23 (2010).

[176]L. J. Cheng and H. C. Chang, "Microscale pH regulation by splitting water," Biomicrofluidics **5**(4), 046502 (2011).

[177]Y. A. Song, R. Melik, A. N. Rabie, A. M. S. Ibrahim, D. Moses, A. Tan, J. Han, and S. J. Lin, "Electrochemical activation and inhibition of neuromuscular systems through modulation of ion concentrations with ion-selective membranes," Nature Mater. **10**, 980–986 (2011).

[178]X. Liu, C. Suo, Y. Zhang, X. Wang, C. Sun, L. Li, and L. Zhang, "Novel modification of Nafion®117 for a MEMS-based micro direct methanol fuel cell (μDMFC)," J. Micromech. Microeng. **16**(9), S226–S232 (2006).

[179]S. J. Kim and J. Han, "Self-sealed vertical polymeric nanoporous-junctions for high-throughput nanofluidic applications," Anal. Chem. **80**(9), 3507–3511 (2008).

[180]J. H. Lee, Y. A. Song, and J. Han, "Multiplexed proteomic sample preconcentration device using surface-patterned ion-selective membrane," Lab Chip **8**(4), 596–601 (2008).

[181]R. Kwak, S. J. Kim, and J. Han, "Continuous-flow biomolecule and cell concentrator by ion concentration polarization," Anal. Chem. **83**(19), 7348–7355 (2011).

[182]J. H. Lee and J. Han, "Concentration-enhanced rapid detection of human chorionic gonadotropin (hCG) on a Au surface using a nanofluidic preconcentrator," Microfluid. Nanofluid. **9**(4), 973–979 (2010).

[183]S. H. Ko, S. J. Kim, L. F. Cheow, L. D. Li, K. H. Kang, and J. Han, "Massively parallel concentration device for multiplexed immunoassays," Lab Chip **11**(7), 1351–1358 (2011).

[184]A. Sarkar and J. Han, "Non-linear and linear enhancement of enzymatic reaction kinetics using a biomolecule concentrator," Lab Chip **11**(15), 2569–2576 (2011).

[185]L. F. Cheow and J. Han, "Continuous signal enhancement for sensitive aptamer affinity probe electrophoresis assay using electrokinetic concentration," Anal. Chem. **83**(18), 7086–7093 (2011).

[186]O. Jännig and N.-T. Nguyen, "A polymeric high-throughput pressure-driven micromixer using a nanoporous membrane," Microfluid. Nanofluid. **10**(3), 513–519 (2010).

[187]S. P. Adiga, C. Jin, L. A. Curtiss, N. A. Monteiro-Riviere, and R. J. Narayan, "Nanoporous membranes for medical and biological applications," Wiley Interdiscip. Rev. Nanomed. Nanobiotechnol. **1**(5), 568–581 (2009).

[188]S. K. Vajandar, D. Xu, D. A. Markov, J. P. Wikswo, W. Hofmeister, and D. Li, "SiO₂-coated porous anodic alumina membranes for high flow rate electroosmotic pumping," Nanotechnology **18**(27), 275705 (2007).

[189]M. Ali, P. Ramirez, S. Mafe, R. Neumann, and W. Ensinger, "A pH-tunable nanofluidic diode with a broad range of rectifying properties," ACS Nano **3**(3), 603–608 (2009).

[190]H. Uehara, M. Kakiage, M. Sekiya, D. Sakuma, T. Yamonobe, N. Takano, A. Barraud, E. Meurville, and P. Ryser, "Size-selective diffusion in nanoporous but flexible membranes for glucose sensors," ACS Nano **3**(4), 924–932 (2009).

[191]F. Li, L. Zhang, and R. M. Metzger, "On the growth of highly ordered pores in anodized aluminum Oxide" Chem. Mater. **10**(9), 2470–2480 (1998).

[192]S. D. Alvarez, C. P. Li, C. E. Chiang, I. K. Schuller, and M. J. Sailor, "A label-free porous alumina interferometric immunosensor," ACS Nano **3**(10), 3301–3307 (2009).

[193]X. Wang and S. Smirnov, "Label-free DNA sensor based on surface charge modulated ionic conductance," ACS Nano **3**(4), 1004–1010 (2009).

[194]S. J. Li, J. Li, K. Wang, C. Wang, J. J. Xu, H. Y. Chen, X. H. Xia, and Q. Huo, "A nanochannel array-based electrochemical device for quantitative label-free DNA analysis," ACS Nano **4**(11), 6417–6424 (2010).

[195]S. Lee, M. Park, H. S. Park, Y. Kim, S. Cho, J. H. Cho, J. Park, and W. Hwang, "A polyethylene oxide-functionalized self-organized alumina nanochannel array for an immunoprotection biofilter," Lab Chip **11**(6), 1049–1053 (2011).

[196]J. Y. Miao, Z. L. Xu, X. Y. Zhang, N. Wang, Z. Y. Yang, and P. Sheng, "Micropumps based on the enhanced electroosmotic effect of aluminum oxide membranes," Adv. Mater. **19**(23), 4234–4237 (2007).

[197]Y.-F. Chen, M.-C. Li, Y.-H. Hu, W.-J. Chang, and C.-C. Wang, "Low-voltage electroosmotic pumping using porous anodic alumina membranes," Microfluid. Nanofluid. **5**(2), 235–244 (2007).

[198]S. Biring, K. T. Tsai, U. K. Sur, and Y. L. Wang, "High speed fabrication of aluminum nanostructures with 10 nm spatial resolution by electrochemical replication," Nanotechnology **19**(35), 355302 (2008).

[199]S. Shin, B. S. Kim, J. Song, H. Lee, and H. H. Cho, "A facile route for the fabrication of large-scale gate-all-around nanofluidic field-effect transistors with low leakage current," Lab Chip **12**(14), 2568–2574 (2012).

[200]T. Xu, G. Zangari, and R. M. Metzger, "Periodic holes with 10 nm diameter produced by grazing Ar+ milling of the barrier laver in hexagonally ordered nanoporous alumina," Nano Lett. **2**(1), 37–41 (2002).

[201]E. Moyen, L. Santinacci, L. Masson, W. Wulfhekel, and M. Hanbucken, "A novel self-ordered sub-10 nm nanopore template for nanotechnology," Adv. Mater. **24**(7), 5094–5098 (2012).

[202]H. Asoh, K. Nishio, M. Nakao, A. Yokoo, T. Tamamura, and H. Masuda, "Fabrication of ideally ordered anodic porous alumina with 63 nm hole periodicity using sulfuric acid," J. Vac. Sci. Technol. B **19**(2), 569–572 (2001).

[203]C. Y. Liu, A. Datta, and Y. L. Wang, "Ordered anodic alumina nanochannels on focused-ion-beam-prepatterned aluminum surfaces," Appl. Phys. Lett. **78**(1), 120–122 (2001).

[204]C. Y. Peng, C. Y. Liu, N. W. Liu, H. H. Wang, A. Datta, and Y. L. Wang, "Ideally ordered 10 nm channel arrays grown by anodization of focused-ion-beam patterned aluminum," J. Vac. Sci. Technol. B **23**(2), 559–562 (2005).

[205]N. W. Liu, A. Datta, C. Y. Liu, and Y. L. Wang, "High-speed focused-ion-beam patterning for guiding the growth of anodic alumina nanochannel arrays," Appl. Phys. Lett. **82**(8), 1281–1283 (2003).

[206]N. W. Liu, A. Datta, C. Y. Liu, C. Y. Peng, H. H. Wang, and Y. L. Wang, "Fabrication of anodic-alumina films with custom-designed arrays of nanochannels," Adv. Mater. **17**(2), 222–225 (2005).

[207]N. W. Liu, C. Y. Liu, H. H. Wang, C. F. Hsu, M. Y. Lai, T. H. Chuang, and Y. L. Wang, "Focused–ion-beam-based selective closing and opening of anodic alumina nanochannels for the growth of nanowire arrays comprising multiple elements," Adv. Mater. **20**(13), 2547–2551 (2008).

[208]P. Y. Apel, "Track etching technique in membrane technology," Radiat. Meas. **34**, 559–566 (2001).

[209]M. Ali, Ph.D. dissertation, der Technischen Universitat Darmstadt, 2009.

[210]L. Wen and L. Jiang, "Bio-inspired smart gating nanochannels based on polymer films," Sci. China Chem. **54**(10), 1537–1546 (2011).

[211]P. Y. Apel and S. N. Dmitriev, "Micro- and nanoporous materials produced using accelerated heavy ion beams," Adv. Nat. Sci.: Nanosci. Nanotechnol. **2**(1), 013002 (2011).

[212]P. Y. Apel, Y. E. Korchev, Z. S. Siwy, R. Spohr, and M. Yoshida, "Diode-like single-ion track membrane prepared by electro-stopping," Nucl. Instrum. Methods Phys. Res. B **184**(3), 337–346 (2001).

[213]P. Y. Apel, I. V. Blonskaya, S. N. Dmitriev, O. L. Orelovitch, A. Presz, and B. A. Sartowska, "Fabrication of nanopores in polymer foils with surfactant-controlled longitudinal profiles," Nanotechnology **18**(30), 305302 (2007).

[214]P. Y. Apel, I. V. Blonskaya, O. L. Orelovitch, B. A. Sartowska, and R. Spohr, "Asymmetric ion track nanopores for sensor technology. Reconstruction of pore profile from conductometric measurements," Nanotechnology **23**(22), 225503 (2012).

[215]S. F. Yu, S. B. Lee, M. Kang, and C. R. Martin, "Size-based protein separations in poly(ethylene glycol)-derivatized gold nanotubule membranes," Nano Lett. **1**(9), 495–498 (2001).

[216]E. N. Gatimu, T. L. King, J. V. Sweedler, and P. W. Bohn, "Three-dimensional integrated microfluidic architectures enabled through electrically switchable nanocapillary array membranes," Biomicrofluidics **1**(2), 021502 (2007).

[217]S. A. Miller, K. C. Kelly, and A. T. Timperman, "Ionic current rectification at a nanofluidic/microfluidic interface with an asymmetric microfluidic system," Lab Chip **8**(10), 1729–1732 (2008).

[218]R. Spohr, C. Zet, B. Eberhard Fischer, H. Kiesewetter, P. Apel, I. Gunko, T. Ohgai, and L. Westerberg, "Controlled fabrication of ion track nanowires and channels," Nucl. Instrum. Methods Phys. Res. B **268**(6), 676–686 (2010).

[219]Q. Yu and Z. Silber-Li, "Measurements of the ion-depletion zone evolution in a micro/nano-channel," Microfluid. Nanofluid. **11**(5), 623–631 (2011).

[220]I. Vlassiouk and Z. S. Siwy, "Nanofluidic diode," Nano Lett. **7** (3), 552–556 (2007).

[221]J. Xue, Y. Xie, Y. Yan, J. Ke, and Y. Wang, "Surface charge density of the track-etched nanopores in polyethylene terephthalate foils," Biomicrofluidics **3**(2), 022408 (2009).

[222]M. Davenport, A. Rodriguez, K. J. Shea, and Z. S. Siwy, "Squeezing ionic liquids through nanopores," Nano Lett. **9**(5), 2125–2128 (2009).

[223]I. Vlassiouk, T. R. Kozel, and Z. S. Siwy, "Biosensing with nanofluidic diodes," J. Am. Chem. Soc. **131**(23), 8211–8220 (2009).

[224]Z. Guo, J. Wang, and E. Wang, "Selective discrimination of small hydrophobic biomolecules based on ion-current rectification in conically shaped nanochannel," Talanta **89**, 253–257 (2012).

[225]A. Mara, Z. S. Siwy, C. Trautmann, J. Wan, and F. Kamme, "An asymmetric polymer nanopore for single molecule detection," Nano Lett. **4** (3), 497–501 (2004).

[226]Q. H. Nguyen, M. Ali, V. Bayer, R. Neumann, and W. Ensinger, "Charge-selective transport of organic and protein analytes through synthetic nanochannels," Nanotechnology **21**(36), 365701 (2010).

[227]X. Hou, W. Guo, F. Xia, F. Q. Nie, H. Dong, Y. Tian, L. Wen, L. Wang, L. Cao, Y. Yang, J. Xue, Y. Song, Y. Wang, D. Liu, and L. Jiang, "A biomimetic potassium responsive nanochannel: G-quadruplex DNA conformational switching in a synthetic nanopore," J. Am. Chem. Soc. **131**(22), 7800–7805 (2009).

[228]E. A. Heins, Z. S. Siwy, L. A. Baker, and C. R. Martin, "Detecting single porphyrin molecules in a conically shaped synthetic nanopore," Nano Lett. **5**(9), 1824–1829 (2005).

[229]J. Wang and C. R. Martin, "A new drug-sensing paradigm based on ion-current rectification in a conically shaped nanopore," Nanomedicine **3**(1), 13–20 (2008).

[230]W. Guo, H. Xia, L. Cao, F. Xia, S. Wang, G. Zhang, Y. Song, Y. Wang, L. Jiang, and D. Zhu, "Integrating ionic gate and rectifier within one solid-state nanopore via modification with dual-responsive copolymer brushes," Adv. Funct. Mater. **20**(20), 3561–3567 (2010).

[231]E. A. Jackson and M. A. Hillmyer, "Nanoporous membranes derived from block copolymers: From drug delivery to water filtration," ACS Nano **4**(7), 3548–3553 (2010).

[232]S. Y. Yang, S. Son, S. Jang, H. Kim, G. Jeon, W. J. Kim, and J. K. Kim, "DNA-functionalized nanochannels for SNP detection," Nano Lett. **11**(3), 1032–1035 (2011).

[233]S. Biring, K. T. Tsai, U. K. Sur, and Y. L. Wang, "Electrochemically replicated smooth aluminum foils for anodic alumina nanochannel arrays," Nanotechnology **19**(1), 015304 (2008).

[234]R. W. Mao, S. K. Lin, and C. S. Tsai, "In situ preparation of an ultra-thin nanomask on a silicon wafer," Nanotechnology **20**(2), 025301 (2009).

[235]C. J. Chang, C. S. Yang, Y. J. Chuang, H. S. Khoo, and F. G. Tseng, "Micro-patternable nanoporous polymer integrated with microstructures for molecular filtration," Nanotechnology **19**(36), 365301 (2008).

[236]D. J. Norris, E. G. Arlinghaus, L. Meng, R. Heiny, and L. E. Scriven, "Opaline photonic crystals: How does self-assembly work?," Adv. Mater. **16**(16), 1393–1399 (2004).

[237]J. D. Joannopoulos, P. R. Villeneuve, and S. Fan, "Photonic crystals: Putting a new twist on light," Nature **386**(6621), 143–149 (1997).

[238]J. H. Holtz and S. A. Asher, "Polymerized colloidal crystal hydrogel films as intelligent chemical sensing materials," Nature **389**(6653), 829–832 (1997).

[239]O. D. Velev and E. W. Kaler, "Structured porous materials via colloidal crystal templating: From inorganic oxides to metals," Adv. Mater. **12**(7), 531–534 (2000).

[240]Y. Zeng and D. J. Harrison, "Self assemble colloidal arrays as three dimensional nanofluidic sieves for separation of bio-molecules on microchips," Anal. Chem. **79**(6), 2289–2295 (2007).

[241]C.-W. Kuo, J.-Y. Shiu, K. H. Wei, and P. Chen, "Monolithic integration of well-ordered nanoporous structures in the microfluidic channels for bioseparation," J. Chromatogr. A **1162**(2), 175–179 (2007).

[242]Y. Zeng, M. He, and D. J. Harrison, "Microfluidic self-patterning of large-scale crystalline nanoarrays for high-throughput continuous DNA fractionation," Angew. Chem., Int. Ed. **47**(34), 6388–6391 (2008).

[243]S. H. Yazdi and I. M. White, "A nanoporous optofluidic microsystem for highly sensitive and repeatable surface enhanced Raman spectroscopy detection," Biomicrofluidics **6**(1), 014105 (2012).

[244]Z. Chen, Y. Wang, W. Wang, and Z. Li, "Nanofluidic electrokinetics in nanoparticle crystal," Appl. Phys. Lett. **95**(10), 102105 (2009).

[245]J. Chen, P.-C. Huang, and M.-G. Lin, "Analysis and experiment of capillary valves for microfluidics on a rotating disk," Microfluid. Nanofluid. **4**(5), 427–437 (2008).

[246]E. Choi, K. Kwon, S. J. Lee, D. Kim, and J. Park, "In-situ self-assembled colloidal crystals within microchannels using one step stemping for direct seawater desalination by ion concentration polarization," in *Proceedings of the 25th International Conference on Micro Electro Mechanical Systems* (IEEE, 2012), pp. 1313–1315.

[247]W. Shen, M. Li, C. Ye, L. Jiang, and Y. Song, "Direct-writing colloidal photonic crystal microfluidic chips by inkjet printing for label-free protein detection," Lab Chip **12**(17), 3089–3095 (2012).

[248]Y. Lei, F. Xie, W. Wang, W. Wu, and Z. Li, "Suspended nanoparticle crystal (S-NPC): A nanofluidics-based, electrical read-out biosensor," Lab Chip **10**(18), 2338–2340 (2010).

[249]Y. Lei, W. Wang, W. Wu, and Z. Li, "Nanofluidic diode in a suspended nanoparticle crystal," Appl. Phys. Lett. **96**(26), 263102 (2010).

[250]M. Zheng, Y. Lei, W. Wang, W. Wu, and Z. Li, "Current rectification in heterogeneous nanoparticle crystals," in The International Symposium on Microchemistry and Microsystems (ISMM), Seoul, Korea, 2–4 June, 2011.

[251]L. Zhang, F. Gu, L. Tong, and X. Yin, "Simple and cost-effective fabrication of two-dimensional plastic nanochannels from silica nanowire templates," Microfluid. Nanofluid. **5**(6), 727–732 (2008).

[252]D. A. Czaplewski, J. Kameoka, R. Mathers, G. W. Coates, and H. G. Craighead, "Nanofluidic channels with elliptical cross sections formed using a nonlithographic process," Appl. Phys. Lett. **83**(23), 4836–4838 (2003).

[253]K. S. Chu, S. Kim, H. Chung, J. H. Oh, T. Y. Seong, B. H. An, Y. K. Kim, J. H. Park, Y. R. Do, and W. Kim, "Fabrication of monolithic polymer nanofluidic channels using nanowires as sacrificial templates," Nanotechnology **21**(42), 425302 (2010).

[254]S. Xu and Y. Zhao, "Monolithic fabrication of nanochannels using core–sheath nanofibers as sacrificial mold," Microfluid. Nanofluid. **11**(3), 359–365 (2011).

[255]W. Gong, J. Xue, Q. Zhuang, X. Wu, and S. Xu, "Fabrication of nanochannels with water-dissolvable nanowires," Nanotechnology **21**(19), 195302 (2010).

[256]U. Vermesh, J. W. Choi, O. Vermesh, R. Fan, J. Nagarah, and J. R. Heath, "Fast nonlinear ion transport via field-induced hydrodynamic slip in sub-20-nm hydrophilic nanofluidic transistors," Nano Lett. **9**(4), 1315–1319 (2009).

[257]M. K. Shin, S. K. Kim, H. Lee, S. I. Kim, and S. J. Kim, "The fabrication of polymeric nanochannels by electro-spinning," Nanotechnology **19**(19), 195304 (2008).

[258]B. J. Hinds, N. Chopra, T. Rantell, R. Andrews, V. Gavalas, and L. G. Bachas, "Aligned multiwalled carbon nanotube membranes," Science **303**(5654), 62–65 (2004).

[259]N. R. Scruggs, J. W. F. Robertson, J. J. Kasianowicz, and K. B. Migler, "Rectification of the ionic current through carbon nanotubes by electrostatic assembly of polyelectrolytes," Nano Lett. **9**(11), 3853–3859 (2009).

[260]R. Fan, R. Karnik, M. Yue, D. Li, A. Majumdar, and P. Yang, "DNA translocation in inorganic nanotubes," Nano Lett. **5**(9), 1633–1637 (2005).

[261]R. Yan, W. Liang, R. Fan, and P. Yang, "Nanofluidic diodes based on nanotube heterojunctions," Nano Lett. **9**(11), 3820–3825 (2009).

[262]H. Liu, J. He, J. Tang, P. Pang, D. Cao, P. Krstic, S. Joseph, S. Lindsay, and C. Nuckolls, "Translocation of single-stranded DNA through single-walled carbon nanotubes," Science **327**(5961), 64–67 (2010).

[263]P. Pang, J. He, J. H. Park, P. S. Krstic, and S. Lindsay, "Origin of giant ionic currents in carbon nanotube channels," ACS Nano **5**(9), 7277–7283 (2011).

[264]R. Fan, Y. Wu, D. Li, M. Yue, A. Majumdar, and P. Yang, "Fabrication of silica nanotube arrays from vertical silicon nanowire templates," J. Am. Chem. Soc. **125**(18), 5254–5255 (2003).

[265]J. Oh, G. Kim, D. Mattia, and H. Noh, "A novel technique for fabrication of micro- and nanofluidic device with embedded single carbon nanotube," Sens. Actuators B **154**(1), 67–72 (2011).

[266]X. Qin, Q. Yuan, Y. Zhao, S. Xie, and Z. Liu, "Measurement of the rate of water translocation through carbon nano-tubes," Nano Lett. **11**(5), 2173–2177 (2011).

[267]A. Noy, H. G. Park, F. Fornasiero, J. K. Holt, C. P. Grigoropoulos, and O. Bakajin, "Nanofluidics in carbon nanotubes," Nano Today **2**(6), 22–29 (2007).

[268]J. Goldberger, R. Fan, and P. Yang, "Inorganic nanotubes: A novel platform for nanofluidics," Acc. Chem. Res. **39**(4), 239–248 (2006).

[269]C. Wang, J. Ouyang, H. L. Gao, H. W. Chen, J. J. Xu, X. H. Xia, and H. Y. Chen, "UV-ablation nanochannels in micro/nanofluidics devices for biochemical analysis," Talanta **85**(1), 298–303 (2011).

[270]C. Wang, J. Ouyang, D. K. Ye, J. J. Xu, H. Y. Chen, and X. H. Xia, "Rapid protein concentration, efficient fluorescence labeling and purification on a micro/nanofluidics chip," Lab Chip **12**(15), 2664–2671 (2012).

[271]X. Hu, Q. He, X. Zhang, and H. Chen, "Fabrication of fluidic chips with 1-D nanochannels on PMMA substrates by photoresist-free UV-lithography and UV-assisted low-temperature bonding," Microfluid. Nanofluid. **10**(6), 1223–1232 (2010).

[272]D. Huh, K. L. Mills, X. Zhu, M. A. Burns, M. D. Thouless, and S. Takayama, "Tuneable elastomeric nanochannels for nanofluidic manipulation," Nature Mater. **6**(6), 424–428 (2007).

[273]K. L. Mills, D. Huh, S. Takayama, and M. D. Thouless, "Instantaneous fabrication of arrays of normally closed, adjustable, and reversible nanochannels by tunnel cracking," Lab Chip **10**(12), 1627–1630 (2010).

[274]B. Y. Xu, J. J. Xu, X. H. Xia, and H. Y. Chen, "Large scale lithography-free nano channel array on polystyrene," Lab Chip **10**(21), 2894–2901 (2010).

[275]H. Yu, Y. Lu, Y. G. Zhou, F. B. Wang, F. Y. He, and X. H. Xia, "A simple, disposable microfluidic device for rapid protein concentration and purification via direct-printing," Lab Chip **8**(9), 1496–1501 (2008).

[276]J.-M. Li, C. Liu, X. Ke, Z. Xu, Y.-J. Duan, M. Li, K.-P. Zhang, and L.-D. Wang, "Microchannel refill: A new method for fabricating 2D nanochannels in polymer substrates," Lab Chip **12**(20), 4059–4062 (2012).

[277]G. G. Dougherty, A. A. Pisano, and T. Sands, "Processing and morphology of permeable polycrystalline silicon thin films," J. Mater. Res. **17**(09), 2235–2242 (2011).

[278]C. C. Striemer, T. R. Gaborski, J. L. McGrath, and P. M. Fauchet, "Charge- and size-based separation of macromolecules using ultrathin silicon membranes," Nature **445**(7129), 749–753 (2007).

[279]D. H. Choi, Y. D. Han, B. K. Lee, S. J. Choi, H. C. Yoon, D. S. Lee, and J. B. Yoon, "Use of a columnar metal thin film as a nanosieve with sub-10 nm pores," Adv. Mater. **22**(32), 4408–4413 (2012).

[280]Z. Y. Wu, C. Y. Li, X. L. Guo, B. Li, D. W. Zhang, Y. Xu, and F. Fang, "Nanofracture on fused silica microchannel for Donnan exclusion based electrokinetic stacking of biomolecules," Lab on a Chip **12**(18), 3408–3412 (2012).

[281]S. M. Kim, M. A. Burns, and E. F. Hasselbrink, "Electrokinetic protein preconcentration using a simple glass/poly(dimethylsiloxane) microfluidic chip," Anal. Chem. **78**(14), 4779–4785 (2006).

[282]C. Wang, S. J. Li, Z. Q. Wu, J. J. Xu, H. Y. Chen, and X. H. Xia, "Study on the kinetics of homogeneous enzyme reactions in a micro/nanofluidics device," Lab Chip **10**(5), 639–646 (2010).

[283]S. M. Park, Y. S. Huh, H. G. Craighead, D. Erickson, "A method for nanofluidic device prototyping using elastomeric collapse," Proc. Natl. Acad. Sci. U.S.A. **106**(37), 15549–15554 (2009).

[284]K.-F. Lo and Y.-J. Juang, "Fabrication of long poly(dimethyl siloxane) nanochannels by replicating protein deposit from confined solution evaporation," Biomicrofluidics **6**(2), 026504 (2012).

[285]L. J. Steinbock, O. Otto, C. Chimerel, J. Gornall, and U. F. Keyser, "Detecting DNA folding with nanocapillaries," Nano Lett. **10**(7), 2493–2497 (2010).

[286]B. Yalizay, T. Ersoy, B. Soylu, and S. Akturk, "Fabrication of nanometer-size structures in metal thin films using femtosecond laser Bessel beams," Appl. Phys. Lett. **100**(3), 031104 (2012).

[287]P. Utko, F. Persson, A. Kristensen, and N. B. Larsen, "Injection molded nanofluidic chips: Fabrication method and functional tests using single-molecule DNA experiments," Lab Chip **11**(2), 303–308 (2011).

[288]J. J. Kasianowicz, E. Brandin, D. Branton, and D. W. Deamer, "Characterization of individual polynucleotide molecules using a membrane channel," Proc. Natl. Acad. Sci. U.S.A. **93**, 13770–13773 (1996).

[289]L. Song, M. R. Hobaugh, C. Shustak, S. Cheley, H. Bayley, and J. E. Gouaux, "Structure of staphylococcal alphahemolysin, a heptameric transmembrane pore," Science **274**(5294), 1859–1866 (1996).

[290]R. F. Purnell and J. J. Schmidt, "Discrimination of single base substitutions in a DNA strand immobilized in a biological nanopore," ACS Nano **3**(9), 2533–2538 (2009).

[291]Y. Wang, D. Zheng, Q. Tan, M. X. Wang, and L. Q. Gu, "Nanopore-based detection of circulating microRNAs in lung cancer patients," Nat. Nanotechnol. **6**(10), 668–674 (2011).

[292]L. Movileanu, S. Howorka, O. Braha, and H. Bayley, "Detecting protein analytes that modulate transmembrane movement of a polymer chain within a single protein pore," Nat. Biotechnol. **18**, 1091–1095 (2000).

[293]D. Rotem, L. Jayasinghe, M. Salichou, and H. Bayley, "Protein detection by nanopores equipped with aptamers," J. Am. Chem. Soc. **134**(5), 2781–2787 (2012).

[294]S. Howorka, L. Movileanu, O. Braha, and H. Bayley, "Kinetics of duplex formation for individual DNA strands within a single protein nanopore," Proc. Natl. Acad. Sci. U.S.A. **98**(23), 12996–13001 (2001).

[295]H. Miedema, M. Vrouenraets, J. Wierenga, W. Meijberg, G. Robillard, and B. Eisenberg, "A biological porin engineered into a molecular, nanofluidic diode," Nano Lett. **7**(9), 2886–2891 (2007).

[296]T. Z. Butler, M. Pavlenok, I. M. Derrington, M. Niederweis, and J. H. Gundlach, "Single-molecule DNA detection with an engineered MspA protein nanopore," Proc. Natl. Acad. Sci. U.S.A. **105**(52), 20647–20652 (2008).

[297]A. Khoutorsky, A. Heyman, O. Shoseyov, and M. E. Spira, "Formation of hydrophilic nanochannels in the membrane of living cells by the ringlike stable protein-SP1," Nano Lett. **11**(7), 2901–2904 (2011).

[298]H. Bayley and L. Jayasinghe, "Functional engineered channels and pores (Review)," Mol. Membr. Biol. **21**(4), 209–220 (2004).

[299]L. J. Cheng and L. J. Guo, "Ionic current rectification, breakdown, and switching in heterogeneous oxide nanofluidic devices," ACS Nano **3**(3), 575–584 (2009.

[300]B. Arkles, "Tailoring surfaces with silanes," CHEMTECH **7**, 766–778 (1977).

[301]P. Mao, Master's thesis, "Fabrication and characterization of nanofluidic channels for studying molecular dynamics in confined environments" (Massachusetts Institute of Technology, 2005).

[302]A. Eitan, K. Jiang, D. Dukes, R. Andrews, and L. S. Schadler, "Surface modification of multiwalled carbon nanotubes: Toward the tailoring of the interface in polymer composites," Chem. Mater. **15**(16), 3198–3201 (2003).

[303]J. L. Bahr and J. M. Tour, "Covalent chemistry of single-wall carbon nanotubes," J. Mater. Chem. **12**(7), 1952–1958 (2002).

[304]V. Georgakilas, K. Kordatos, M. Prato, D. M. Guldi, M. Holzinger, and A. Hirsch, "Organic functionalization of carbon nanotubes," J. Am. Chem. Soc. **124**(5), 760–761 (2002).

[305]N. N. Li, A. G. Fane, W. S. Winston, and T. Matsuura, *Advanced Membrane Technology and Applications* (John Wiley & Sons, Inc., 2008).

[306]G. F. Schneider and C. Dekker, "DNA sequencing with nanopores," Nat. Biotechnol. **30**(4), 326–328 (2012).

[307]L. Q. Gu and J. W. Shim, "Single molecule sensing by nanopores and nanopore devices," Analyst **135**, 441–451 (2010).

[308]R. Spohr, "Status of ion track technology—Prospects of single tracks," Radiat. Meas. **40**, 191–202 (2005).

[309]R. Fan, S. Huh, R. Yan, J. Arnold, and P. Yang, "Gated proton transport in aligned mesoporous silica films," Nature Mater. **7**(4), 303–307 (2008).

[310]Y. C. Wang, A. L. Stevens, and J. Han, "Million-fold preconcentration of proteins and peptides by nanofluidic filter," Anal. Chem. **77**(14), 4293–4299 (2005).

[311]J. Fu, P. Mao, and J. Han, "Nanofilter array chip for fast gel-free biomolecule separation," Appl. Phys. Lett. **87**, 263902 (2005).

[312]D. Stein, M. Kruithof, and C. Dekker, "Concentration polarization and nonlinear electrokinetic flow near a nanofluidic channel," Phys. Rev. Lett. **99**(4), 044501 (2007).

[313]J. Yeom, Y. Wu, J. C. Selby, and M. A. Shannon, "Maximum achievable aspect ratio in deep reactive ion etching of silicon due to aspect ratio dependent transport and the microloading effect," J. Vac. Sci. Technol. B **23**(6), 2319–2329 (2005).

[314]E. A. Strychalski, S. M. Stavis, and H. G. Craighead, "Non-planar nanofluidic devices for single molecule analysis fabricated using nanoglassblowing," Nanotechnology **1931**, 315301 (2008).

[315]S. Howorka and Z. S. Siwy, "Nanopores as protein sensors," Nat. Biotechnol. **30**(6), 506–507 (2012).

[316]B. W. Ward, J. A. Notte, and N. P. Economou, "Helium ion microscope: A new tool for nanoscale microscopy and metrology," J. Vac. Sci. Technol. B **24**, 2871–2874 (2006).

[317]V. Sidorkin, E. van Veldhoven, E. van der Drift, P. Alkemade, H. Salemink, and D. Maas, "Sub-10-nm nanolithography with a scanning helium beam," J. Vac. Sci. Technol. B **27**(4), L18–L20 (2009).

[318]F. Xie, Y. Wang, W. Wang, Z. Li, G. Yossifon, and H.-C. Chang, "Preparation of rhombus-shaped micro/nanofluidic channels with dimensions ranging from hundred nanometers to several micrometers," J. Nanosci. Nanotechnol. **10**(11), 7277–7281 (2010).

[319]H. Daiguji, N. Tatsumi, S. Kataoka, and A. Endo, "One-dimensional alignment of SBA-15 films in microtrenches," Langmuir **25**(19), 11221–11224 (2009).

[320]H. Daiguji, D. Nakayama, A. Takahashi, S. Kataoka, and A. Endo, "Ion transport in mesoporous silica thin films," in Proceedings of the ASME/JSME 2011 8th Thermal Engineering Joint Conference, Honolulu, Hawaii, USA, 13–17 March 2011.

[321]H. Daiguji, J. Hwang, A. Takahashi, S. Kataoka, and A. Endo, "Ion transport in mesoporous silica SBA-16 thin films with 3D cubic structures," Langmuir **28**(7), 3671–3677 (2012).